Science of the Total Environment 865 (2023) 161134

Contents lists available at ScienceDirect

Science of the Total Environment

journal homepage: www.elsevier.com/locate/scitotenv

Future air quality and premature mortality in Korea

Yujin J. Oak [a], Rokjin J. Park [a,*], Jong-Tae Lee [b,c], Garam Byun [c]

[a] School of Earth and Environmental Sciences, Seoul National University, Seoul, South Korea
[b] School of Health Policy and Management, College of Health Science, Korea University, Seoul, South Korea
[c] Interdisciplinary Program in Precision Public Health, Korea University, Seoul, South Korea

HIGHLIGHTS

- We investigated future changes in pollutant concentrations and attributable premature mortality in Korea.
- SSP1 (strong emissions control) and SSP3 (mild emissions control) scenarios were considered for future simulations.
- O_3 will decrease in a NO_x-limited regime under SSP1, but increase in a VOC-limited regime under SSP3.
- NO_2, SO_2, $PM_{2.5}$ and its components will generally decrease under SSP1 and SSP3.
- BSOA contribution to total $PM_{2.5}$ will increase in the future.
- Premature mortality due to air pollutants will decrease by 95 % and 22 % under SSP1 and SSP3, respectively.

GRAPHICAL ABSTRACT

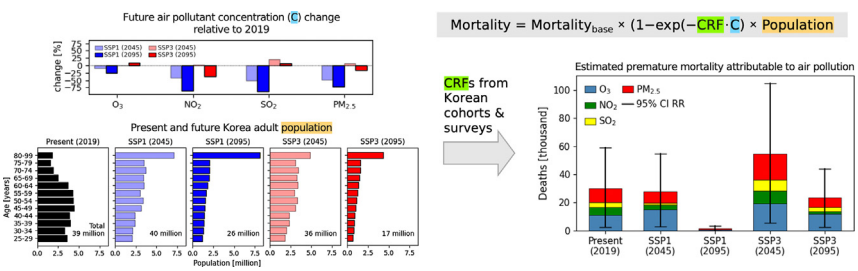

ARTICLE INFO

Editor: Hai Guo

Keywords:
Chemical transport model
Air pollution
Premature mortality
Shared Socioeconomic Pathways (SSPs)

ABSTRACT

We simulate air quality in Korea for the present, the near-term, and the long-term future conditions under the Shared Socioeconomic Pathways (SSP1: most sustainable pathway with strong emissions control, SSP3: most challenging pathway with mild emissions control) using a chemical transport model. Simulated future concentrations of NO_2, SO_2, and fine particulate matter ($PM_{2.5}$), show, in general, lower values compared to the present with varying degrees depending on SSP scenarios. Significant reductions in precursor emissions result in a decrease in O_3 concentrations under a NO_x-limited environment in the long-term future under SSP1. Under SSP3, O_3 increases in the future under a VOC-limited regime, driven by increased CH_4 levels and biogenic VOC emissions under the warming climate. Concentrations of $PM_{2.5}$ and its components, including sulfate, nitrate, ammonium, and organic aerosols (OA), generally decrease in the long-term future under both scenarios. However, the contribution of biogenic secondary OA (BSOA) to $PM_{2.5}$ will increase in the future. Simulated results are used to estimate cardiorespiratory mortality changes with concentration-response factors from epidemiologic studies in Korea based on national health surveys and Korean cohorts, using projected population structures from the SSP database. The cardiorespiratory health burden of long-term exposure to O_3, NO_2, SO_2, and $PM_{2.5}$ is estimated to be 10,419 (95 % confidence interval: 1271–17,142), 8630 (0–18,713), 3958 (0–9272), and 10,431 (1411–20,643) deaths in 2019. We find that the total cardiorespiratory excess mortality due to air pollutants under SSP1 decreases by 8 % and 95 % in 2045 and 2095, respectively. Under SSP3, excess mortality increases by 80 % in 2045, and decreases by 22 % in 2095, resulting in a substantial difference in the health outcomes depending on the emission scenario. We also find that the BSOA contribution to total $PM_{2.5}$ will differ by region, emphasizing the potential health impact of BSOA on a local scale in the future.

* Corresponding author.
E-mail address: rjpark@snu.ac.kr (R.J. Park).

http://dx.doi.org/10.1016/j.scitotenv.2022.161134
Received 11 October 2022; Received in revised form 22 November 2022; Accepted 19 December 2022
Available online 29 December 2022

1. Introduction

Adverse health effects of long-term exposure to surface air pollutants, including gas phase ozone (O_3), nitrogen dioxide (NO_2), sulfur dioxide (SO_2), and particulate matter (PM; PM_{10} and $PM_{2.5}$) on the human cardiovascular and respiratory systems have been widely addressed by epidemiologic (Crouse et al., 2015; Faustini et al., 2014; Hoek et al., 2013; Huangfu and Atkinson, 2020; Soares and Silva, 2022) and air quality modeling studies (Anenberg et al., 2010; Silva et al., 2016; Xu et al., 2021). The concentration-response factor (CRF) represents the relationship between pollutant exposure and health outcomes, and using an appropriate CRF is essential in estimating the health burden attributable to exposure to air pollutants. Systematic reviews on long-term exposure to pollutants including O_3, NO_2, and PM identified clear evidence of positive associations with cardiorespiratory mortality but also reported large heterogeneities of the CRFs of O_3 and NO_2 identified from various studies across the United States, Europe, Canada, China, and Japan (Chen and Hoek, 2020; Huangfu and Atkinson, 2020).

Despite the high levels of heterogeneity, previous studies have commonly applied CRFs that were mainly based on North American or European cohorts to estimate the health outcomes in other global regions (Park et al., 2020; Silva et al., 2017), including Korea (Kim et al., 2019a; Kim et al., 2019b). Bae and Kwon (2019) reviewed 27 published epidemiologic studies in Korea for the past two decades (1999 to 2018), which reported significant associations between long-term exposure to air pollution and mortality quantified by the relative risks (RR), hazard ratios (HR), and odds ratios (OR), but emphasized the necessity of additional cohort-based studies that can provide a more robust concentration-response relationship. As a follow-up, recent studies (Byun et al., 2021, 2022; Kim et al., 2021) based on Korean cohorts and health surveys have estimated age, cause, and region-specific RRs for use in the estimation of the health burden attributable to long-term exposure to O_3, NO_2, SO_2, and PM in Korea.

While global climate change, associated with changes in both meteorological variables and emissions, is expected to alter surface air quality in the future, most studies found that pollutant level changes in the future are mainly driven by the changes in precursor emissions (Kim et al., 2015; Shim et al., 2020; Thornhill et al., 2021). Several studies have also investigated the impact of future air quality change on global premature mortality (Park et al., 2020; Silva et al., 2017), including in Europe (Orru et al., 2012), the United States (Fann et al., 2014; Tagaris et al., 2009), China (Xu et al., 2021), and India (Chowdhury et al., 2018). Shim et al. (2020) analyzed near-term and long-term future changes in $PM_{2.5}$ concentrations in Korea under the Shared Socioeconomic Pathways (SSPs) simulated by an Earth System Model (UKESM1) and found that $PM_{2.5}$ levels will decrease in all future scenarios except for the SSP3 scenario, which assumes the highest challenges in terms of climate mitigation and adaptation with low priorities in reducing anthropogenic emissions. Kim et al. (2020) investigated the O_3 and $PM_{2.5}$ related health benefits of climate mitigation in 2050 under SSP2 (moderate socioeconomic growth and challenges) and SSP3 in Korea using a regional model (WRF/CMAQ) and CRFs from European (Amann et al., 2008) and American (Jerrett et al., 2009) epidemiological studies. They found that future changes in O_3 and $PM_{2.5}$ attributable mortality relative to 2005 will decrease in both scenarios, but the magnitude of reduction under SSP2 will be larger than that under SSP3 by a factor of two.

Not only the changes in single pollutant concentrations but also the changes in the chemical composition of trace gases and particles in the atmosphere can affect future health outcomes. However, several Earth system models (ESM) used in previous studies and future experiments therein often implemented simplified chemistry schemes for efficiency (Kim et al., 2015; Lee et al., 2022; Thornhill et al., 2021). Therefore, despite its computational cost, a more complex air quality model that can reflect both the anthropogenic and natural formation and degradation processes of secondary pollutants is necessary for more accurate estimations of future pollutant levels and for understanding the chemical regimes and mechanisms that drive the changes.

In this study, we simulate air quality in Korea for the present (2019) and near-term (2045) and long-term (2095) future conditions under two SSP scenarios (SSP1: the most sustainable pathway with strong emissions control, SSP3: the most challenging pathway with mild emissions control) using GEOS-Chem, a 3-D global chemical transport model (CTM) which simulates the primary and secondary formation and transport of gases and aerosols in the atmosphere. In particular, we use the most suitable approach to simulate gas and particle phase organic chemistry in Korea. Simulated results are used to estimate municipal-level O_3, NO_2, SO_2, and $PM_{2.5}$ attributable cardiorespiratory mortality changes using the CRFs based on recent Korean cohorts and health surveys. We consider future anthropogenic and natural emissions changes under each scenario based on the Coupled Model Intercomparison Project Phase 6 (CMIP6) experiments and Korea's future population and age structures from the SSP database. However, we do not take into account the direct effect of meteorological variables (e.g., wet and dry deposition, wind speed, temperature, humidity, etc.) due to climate change. We first compare future changes in surface O_3, NO_2, SO_2, and $PM_{2.5}$ and its chemical components and quantify the effect of anthropogenic emission reductions and changes in natural emissions on future air quality. We then compare future changes in premature mortality caused by each pollutant and quantify the effect of pollutant concentration change and population structure change on total excess mortality attributable to air pollution, which can provide insight into the health benefits of future regulation policies.

2. Methods

2.1. Air quality simulations

We use a 3-D global CTM, GEOS-Chem version 13.3.4 (Park et al., 2003, 2004), to simulate surface concentrations of air pollutants, including O_3, nitrogen oxides ($NO_x \equiv NO + NO_2$), volatile organic compounds (VOCs), SO_2, and $PM_{2.5}$ in Korea. GEOS-Chem is driven by the NASA Goddard Earth Observing System-forward processing (GEOS-FP) assimilated meteorology provided by the NASA Global Modeling Assimilation Office (GMAO). Global simulations using a 2° latitude by 2.5° longitude horizontal resolution were used to provide boundary and initial conditions for the nested simulations, which cover the East Asian domain (15–55°N, 70–140°E). The nested simulations have a 0.25° latitude by 0.3125° longitude horizontal resolution (Fig. 1) and 47 vertical layers using the hybrid pressure-sigma coordinate system (1013.25–0.010 hPa).

GEOS-Chem simulates >300 chemical species using a detailed tropospheric-stratospheric photochemical mechanism, incorporating several heterogeneous reactions (e.g., HO_2 and O_3 uptake by aerosols), which is coupled with black carbon (BC), primary organic aerosol (POA), secondary inorganic aerosol (SIA $\equiv SO_4^{2-} + NO_3^- + NH_4^+$), and secondary organic aerosol (SOA) simulations (Park et al., 2003, 2004). SIA thermodynamics associated with aerosol liquid water content, acidity, relative humidity, etc., is computed using the ISORROPIA II thermodynamic equilibrium model (Fountoukis and Nenes, 2007). A full description of carbonaceous aerosol (BC, POA, SOA) simulations can be found in Oak et al. (2022) and Pai et al. (2019).

For SOA simulations, we use the "Hodzic" SOA scheme, which uses the volatility basis set (VBS) method with six bins and updated yield parameters that simulate high-NO_x and low-NO_x pathways of SOA formation (Hodzic et al., 2016), and SOA aging to simulate functionalization (Jo et al., 2013), which was found to be the most suitable approach in reproducing the formation and photochemical processing of observed SOA in Korea (Oak et al., 2022). This SOA scheme simulates SOA formation from aromatic VOCs (AVOCs), semi/intermediate VOCs (S/IVOCs), and terpenes. We estimate S/IVOCs emissions by summing up 50 % of primary OC (POC) and 20 % of non-methane volatile organic compounds (NMVOCs) emissions from anthropogenic and biomass burning sources, as traditional inventories do not include these emissions (Jathar et al., 2014). We use an explicit mechanism for SOA derived by isoprene (Marais et al., 2016) instead of the VBS based method by Hodzic et al.

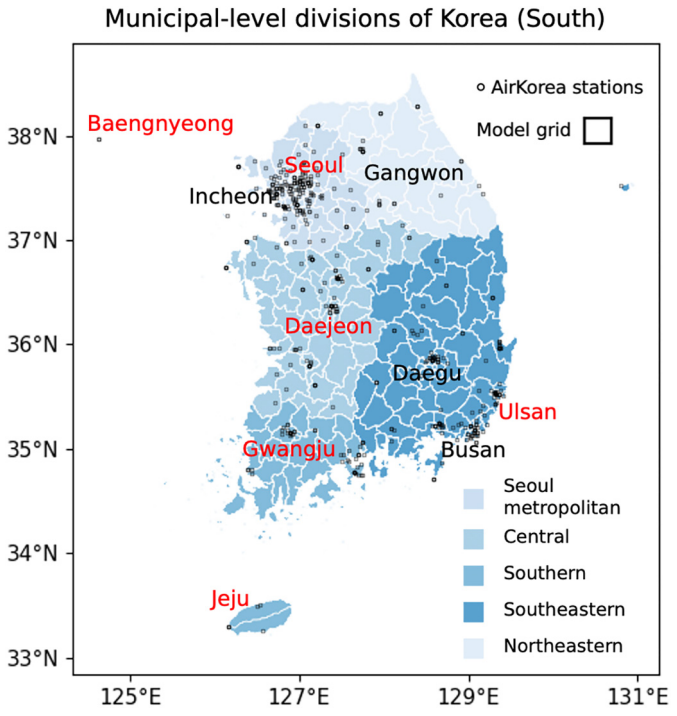

Fig. 1. Map of municipal-level divisions of Korea with geographic locations of major cities denoted in black, AirKorea monitoring stations in black open circles, and six $PM_{2.5}$ ground sites denoted in red. The model grid box size is shown for comparison.

(2016) and Pye et al. (2010). This method explicitly simulates the formation of low-volatility organics, including isoprene epoxydiol (IEPOX), which undergo irreversible aqueous-phase processes that occur more efficiently on acidic aerosol surfaces (Marais et al., 2016). We define biogenic SOA (BSOA) as the sum of SOA derived by terpenes, simulated using the VBS approach, and by isoprene, simulated using the explicit aqueous-phase mechanism.

We first conduct the baseline simulation for 2019, representing present-day conditions. We use 2019 emissions from the Community Emissions Data System (CEDS) version 2 inventory for anthropogenic emissions (McDuffie et al., 2020), the Model of Emissions of Gases and Aerosols from Nature (MEGAN) version 2.1 for biogenic emissions (Guenther et al., 2012), and the Quick Fire Emissions Dataset (QFED) version 2.5 for biomass burning emissions (Darmenov and da Silva, 2015).

We conduct four additional simulations to compare the near-term and long-term changes under two SSP scenarios: SSP1, the most sustainable pathway with strong emissions control, and SSP3, the least sustainable scenario with mild regulations on anthropogenic emissions. We set the target years for the near-term and long-term future conditions to 2045 and 2095, respectively (Table 1). We fix the meteorological fields to those of 2019 to eliminate the direct effect of meteorological change on pollutants such as wet and dry deposition, wind speed, temperature, humidity, etc., and focus on the changes in emissions and chemical formation. Future changes in land surface types and land use are also fixed to those of 2019. However, we account for future changes in biogenic emissions, which change from the vegetation response to temperature stress and CO_2 inhibition (Cao et al., 2021), and changes in methane (CH_4) concentrations due to climate change by applying scale factors to the present-day biogenic emissions and CH_4 levels based on previous studies (Cao et al., 2021; Saunois et al., 2020; Turnock et al., 2020). For future anthropogenic and biomass burning emissions, we use projected emissions in the CMIP6 and BB4CMIP experiments (Gidden et al., 2019; van Marle et al., 2017). Emission totals of anthropogenic and biomass burning CO, NO_x, SO_2, POA, NMVOCs, and BVOCs (isoprene, monoterpenes, acetone, acetaldehyde, ethene, propene, ethanol, methanol) emissions in Northeast Asia (20–50°N, 100–140°E), and global CH_4 concentrations are summarized in Table 1.

2.2. Premature mortality estimation

Fig. 1 shows each geographical region in Korea. We use provincial-level (Korean; Si-Do) age-specific and cause-specific baseline mortality rates and municipal-level (Korean; Si-Gun-Gu) adult population in Korea for 2019 obtained from the Korean Statistical Information Service (KOSIS) portal (https://kosis.kr/eng/). We select two cardiovascular disease categories: ischemic heart disease (IHD; KCD I20-I25) and other heart diseases (KCD I26-I51), and three respiratory disease categories: acute lower respiratory infection (ALRI; KCD J20-J22, U04), chronic obstructive pulmonary disease (COPD; KCD J40-J47), and other respiratory diseases (KCD J00-J98) for the calculation of premature deaths caused by air pollution.

We assume a log-linear relationship between the RR and long-term exposure to a pollutant, following the work by Anenberg et al. (2010). The relative risk per Δx increase of pollutant concentration is an exponential function, as shown in Eq. (1), where β is the CRF, defined by the slope of the log-linear relation between the RR and pollutant concentration. The health outcome (Mort) is estimated using Eq. (2), where $Mort_{base}$ indicates the baseline mortality rate, Pop indicates the exposed adult (≥25 years) population, and AF is the attributable fraction of the pollutant. If the pollutant concentration (C) is below the threshold (C_{thres}), the AF is set to 0, but if $C \geq C_{thres}$, then the AF is defined as Eq. (3). The threshold values of each pollutant are summarized in Table 2.

$$RR = e^{\beta \Delta x} \tag{1}$$

$$Mort = Mort_{base} \times Pop \times AF \tag{2}$$

$$AF = \frac{RR - 1}{RR} = 1 - \exp(-\beta \Delta C), \text{where} \Delta C = C - C_{thres} \tag{3}$$

To obtain the CRFs, i.e., β, we use Eq. (1) and RRs from recent epidemiologic studies in Korea, which estimated the association between long-term

Table 1
Annual emission totals in Northeast Asia and global CH_4 concentrations.

Category	Species	Present (2019)	SSP1 (2045)	SSP1 (2095)	SSP3 (2045)	SSP3 (2095)
Anthropogenic emissions [Tg]	CO	156	71	25	145	72
	NO_x	14.1	6.9	1.9	17.2	9.7
	SO_2	14.0	3.0	0.3	15.6	11.2
	POA	2.64	1.06	0.82	2.87	1.78
	NMVOCs	23.4	10.0	6.1	23.1	21.8
Biomass burning emissions [Tg]	CO	0.19	0.21	0.18	0.32	0.48
	POA	0.048	0.061	0.056	0.088	0.122
	NMVOCs	0.0014	0.0016	0.0014	0.0021	0.0028
Biogenic emissions [Tg] [a]		21.8	24.4	23.6	24.6	29.1
Global CH_4 [ppbv] [b]		1850	1580	2400	1080	3300

[a] Cao et al. (2021).
[b] Saunois et al. (2020), Turnock et al. (2020).

Table 2
RRs with 95 % confidence intervals (95 % CI) for cardiovascular and respiratory mortality per Δx increase of pollutants in Korea.

Pollutant	Threshold	Δx	Cardiovascular disease	Respiratory disease	Region	Reference
Annual mean MDA8[a] O_3	33.3 ppbv (Anenberg et al., 2010)	10 ppbv	1.27 (1.04–1.55)	1.43 (1.04–1.96)	Nationwide	Byun et al. (2022)
Annual mean NO_2	5.3 ppbv (10 μg m^{-3}; WHO guideline)	11.41 ppbv	1.312 (0.949–1.814)	0.903 (0.625–1.303)	Nationwide	Kim et al. (2021)
Annual mean SO_2	2 ppbv (Kim et al., 2021)	2.09 ppbv	1.200 (0.960–1.500)	0.817 (0.589–1.133)	Nationwide	Kim et al. (2021)
Annual mean $PM_{2.5}$	5 μg m^{-3} (WHO guideline)	10 μg m^{-3}	1.244 (1.041–1.487)	1.166 (0.943–1.440)	Seoul metropolitan[b]	Byun et al. (2021)
			1.211 (0.952–1.540)	1.466 (1.125–1.912)	Central[c]	
			0.840 (0.511–1.382)	0.905 (0.524–1.561)	Southern[d]	
			1.053 (0.927–1.195)	1.171 (0.993–1.382)	Southeastern[e]	
			1.136 (0.739–1.746)	1.118 (0.705–1.774)	Northeastern[f]	

[a] Daily maximum 8-hour average.
[b] Seoul, Incheon, Gyeonggi province.
[c] Daejeon, Sejong, North Chungcheong province, South Chungcheong province, North Jeolla province.
[d] Gwangju, South Jeolla province, Jeju.
[e] Busan, Ulsan, Daegu, North Gyeongsang province, South Gyeongsang province.
[f] Gangwon province.

exposure to O_3, NO_2, SO_2, PM_{10}, and cardiorespiratory mortality using the Korean National Health and Nutritional Examination Survey (KNHANES) (Kim et al., 2021) and the National Health Insurance Service-National Sample Cohort database (Byun et al., 2021, 2022) along with air quality observations. Table 2 summarizes the cause and region-specific RRs and corresponding Δx of each pollutant used in this study.

The RRs of peak O_3 levels in a global meta-analysis review by Huangfu and Atkinson (2020) were 1.10 (95 % CI: 1.03–1.18) and 1.02 (0.99–1.05) for ALRI and respiratory mortality, respectively. The results from Byun et al. (2022), which are used in this study, show larger RRs of 8-hour O_3 in Korea (Table 2). The RRs of NO_2 in the global meta-analysis were 1.03 (1.01–1.04), 1.06 (1.02–1.10), and 1.03 (1.00–1.05) for COPD, ALRI, and respiratory diseases. However, Table 2 shows that long-term exposure to NO_2 has a negative relationship with respiratory mortality in Korea. According to an ecological analysis of long-term exposure to air pollutants and cardiopulmonary mortality in Korea (Hwang et al., 2020), NO_2 showed negative associations with pneumonia, 0.893 (0.861–0.923), and chronic lower respiratory disease, 0.822 (0.780–0.865). Hwang et al. (2020) reported significant associations between cardiovascular diseases and long-term exposure to SO_2, with 1.09 (1.05–1.12) for IHD, but negative associations between respiratory diseases and SO_2, with 0.968 (0.943–0.994) for pneumonia, in Korea, which is consistent with the results from Kim et al. (2021), which are used in this study.

For calculating $PM_{2.5}$-attributable premature mortality, we use RRs estimated for PM_{10} due to the limited amount of long-term $PM_{2.5}$ observations in Korea (Byun et al., 2021). The combined RRs of PM_{10} and $PM_{2.5}$ in a meta-analysis review of approximately 20 studies on various global regions (Chen and Hoek, 2020) were 1.04 (0.99–1.10) and 1.11 (1.09–1.14), respectively, for circulatory diseases. For respiratory diseases, the RRs of PM_{10} and $PM_{2.5}$ were 1.12 (1.06–1.19) and 1.10 (1.03–1.18), respectively. Byun et al. (2021) noted that the RRs obtained from the Korean data are consistent with studies conducted in different countries. However, by incorporating Korean cohorts and PM data, the RRs of $PM_{2.5}$ used in this study represent the local characteristics and differences in PM levels, domestic population, and confounders, including income, drinking, smoking status, physical activity, and obesity.

For the estimation of future premature mortality under the SSPs, we use the 2019 baseline mortality rates. Assuming that the spatial distribution of the municipal-level population in the future is identical to that of 2019, we apply age-specific scale factors provided by the International Institute for Applied Systems Analysis (IIASA) SSP database (https://tntcat.iiasa.ac.at/SspDb) to the 2019 population data for each future scenario and year (KC and Lutz, 2017). Therefore, although future changes in the baseline mortality rates are neglected, we consider the changes in the total population and age structure. Fig. S1 compares the adult population of 25 years and older and the age structure in the present and future scenarios. Population aging will be a common phenomenon under both scenarios, and the adult population will fall dramatically by 2095 under SSP3.

3. Model evaluation for present-day (2019) conditions

In this section, we evaluate GEOS-Chems performance in simulating present-day conditions using hourly surface observations of O_3, NO_2, SO_2, and $PM_{2.5}$ at 419 AirKorea surface monitoring stations (https://www.airkorea.or.kr/eng/) during 2019. As the AirKorea network does not provide speciated $PM_{2.5}$ observations, we compare observed and simulated $PM_{2.5}$ chemical compositions at six supersites (Seoul, Daejeon, Gwangju, Ulsan, Baengnyeong, Jeju), which were provided by the National Institute of Environmental Research (NIER). However, as continuous chemical composition observations at the six ground sites for 2019 were unavailable in this study, we compare the seven-year averaged observations conducted from 2012 to 2018 with 2019 simulations. Locations of the ground observation sites are shown in Fig. 1.

Fig. 2 compares observed and simulated MDA8 (daily maximum 8-hour average) O_3, daytime (06:00–18:00 local time) NO_2, SO_2, and $PM_{2.5}$ at AirKorea stations during 2019. We compare the daytime levels of NO_2, SO_2, and $PM_{2.5}$ to minimize the model-observation bias caused by the shallow nighttime planetary boundary (PBL) height in the model. While Oak et al. (2019) showed that GEOS-Chem underestimates the nighttime PBL by more than a factor of two compared to lidar-derived observations in Korea, this causes a rapid increase in simulated surface pollutant levels after sunset and a sharp decrease after sunrise. Therefore, we select the 06:00–18:00 local time (KST; Korea Standard Time = UTC + 9 h) data for our analysis of NO_2, SO_2, and $PM_{2.5}$ below.

We use the normalized mean bias (NMB), Pearson correlation coefficient (R), and reduced-major-axis (RMA) regression between the observation and model to evaluate model performance. Fig. 2a compares the monthly mean surface timeseries averaged over all AirKorea stations during 2019. The comparison shows that the model-observation biases for O_3, SO_2, and $PM_{2.5}$ are <10 %, but a relatively large bias of −30 % is shown in simulated NO_2 levels. This discrepancy may be attributable to interferences by non-NO_x reactive nitrogen species (NO_z) in the chemiluminescence monitors with molybdenum oxide converters that were used for measuring NO_2 (Dunlea et al., 2007; Reed et al., 2016). Although this interference is difficult to quantify using the available observations in this study, we find that simulated NO_z species, including PANs (peroxy acyl nitrates), nAPNs (non-acyl peroxy nitrates), N_2O_5, HNO_3, HONO, NO_3, and ANs (alkyl nitrates), especially NO_3, show non-negligible surface concentrations during the daytime in Korea. Comparison of the simulated sum of NO_2 and non-NO_x NO_z to measured NO_2 shows a model-observation bias of +16 %. Therefore, we speculate that the magnitude of the bias for simulated NO_2 should lie within the range of −30 % to +16 %. While the model reproduces observed monthly variations of O_3, NO_2, and $PM_{2.5}$, with $R \geq 0.7$, we find that the monthly variation of anthropogenic SO_2 emissions strongly resembles the simulated SO_2 timeseries, resulting in a relatively weak ($R = 0.59$) temporal correlation between observed and simulated monthly mean SO_2 compared to other species. The model generally captures the total

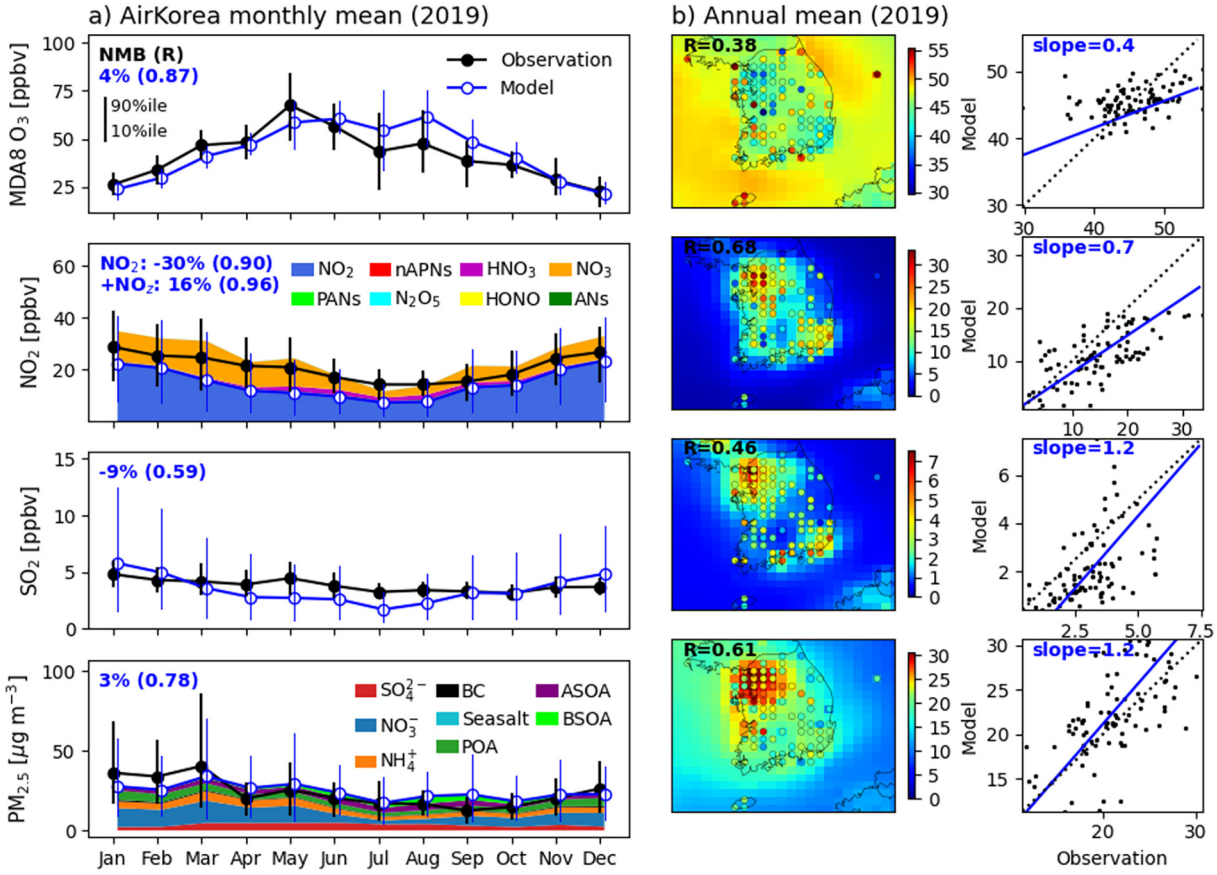

Fig. 2. Observed and simulated a) monthly mean timeseries, b) annual mean spatial distribution and scatterplot comparison of MDA8 O_3, NO_2, SO_2, and $PM_{2.5}$ at AirKorea stations during 2019. Statistics (NMB, R) of model performance are denoted in the upper-left corners. Error bars indicate the 10th and 90th percentile values. Simulated NO_z species and chemical components of $PM_{2.5}$ in column a) are shown in different shades. Overlayed circles in column b) indicate the AirKorea observations regridded and interpolated to the model grid resolution.

amount and monthly variation of observed $PM_{2.5}$, with nitrate aerosols making up the largest portion among the simulated $PM_{2.5}$ components.

Fig. 2b compares the spatial distributions of observed and simulated annual mean surface concentrations of air pollutants. AirKorea observations were regridded and interpolated to match the 0.25° latitude by 0.3125° longitude horizontal resolution for comparison with the model. The simulated spatial distribution of O_3 shows a weak correlation with observations compared to other species. We find that the model overestimates O_3 in the Seoul metropolitan area, which is partly responsible for the RMA regression slope of 0.4. A sensitivity test using different horizontal resolutions in the model showed that simulated surface daytime O_3 decreases by ~2 % when using a finer model (9 km versus 3 km horizontal resolution) in Seoul (Hyeonmin Kim, personal communication, November 13, 2022), implying that the spatial resolution of the model can affect O_3 chemistry. The spatial correlation between observed and simulated SO_2 concentrations is lower ($R = 0.46$) compared to previous model simulations in Korea ($R = 0.74$) (Park et al., 2021). A comparison of the KORUSv5 2016 emissions inventory used in Park et al. (2021) and CEDSv2 2019, which was used in this study, implies that the inaccurate representation of power plants and petrochemical complexes located along the western and southern coasts of the Korean peninsula, which serve as large point sources of SO_2 emissions in Korea (Chong et al., 2020), is the main contributor to the discrepancy. The spatial distributions of observed NO_2 and $PM_{2.5}$ are well captured by the model, showing high values in urban and industrial regions.

Fig. 3 compares observed (2012–2018 mean) and simulated (2019) monthly mean surface timeseries of the major $PM_{2.5}$ chemical components: SIA, BC or elemental carbon (EC), and organic aerosols (OA) at six ground sites. As the model simulates POC, we multiply an organic aerosol to organic carbon ratio (OA/OC) of 1.3 for the conversion of POC to POA based on observations in East Asia (Kim et al., 2017; Kim et al., 2018a; Philip et al., 2014), and define modeled OA as the sum of POA and SOA (Oak et al., 2022). We apply an OA/OC of 1.67 for January and October (Kim et al., 2017), and 1.82 for April and July (Kim et al., 2018a) to the observed OC concentrations for comparison with the model.

We find that simulated SIA is overestimated compared to the seven-year average observations, especially during spring, due to the model's large nitrate (NO_3^-) composition (Fig. 2a). Nitrate overestimation in East Asia has been commonly reported by air quality modeling studies (Choi et al., 2019; Luo et al., 2020; Park et al., 2021; Travis et al., 2022; Zhai et al., 2022). These studies suggest several missing sinks of nitrate and nitric acid (HNO_3) in the model, including photolysis, dry and wet deposition, and uptake on anthropogenic coarse PM. We find that the model-observation bias for monthly mean BC is 10 %, and the model successfully simulates the monthly variation of observed BC. Simulated OA averaged at the six sites overestimates observations by 20 %, and the model fails to capture the seasonal variation of observed OA ($R = -0.63$). This is mainly due to the high bias of SOA during summer, likely caused by overestimated SOA aging (Oak et al., 2022) and BSOA formation in the model. The conversion of measured OC to OA using constant OA/OC values may also serve as uncertainty that causes the bias.

4. Future changes in air pollutants under the SSPs

4.1. Gas species

Table 3 compares simulated annual mean pollutant concentrations in 2019 and the near-term and long-term future under the SSP1 and SSP3 scenarios. Fig. 4a compares the relative difference in annual mean

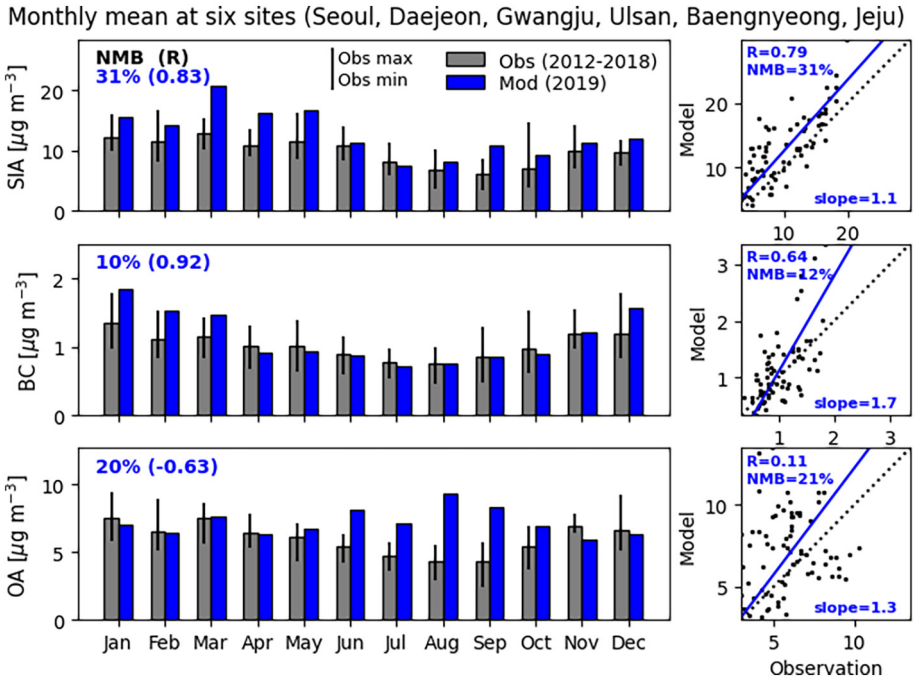

Fig. 3. Observed (2012–2018 mean) and simulated (2019) monthly mean timeseries of major $PM_{2.5}$ chemical components at six supersites (Seoul, Daejeon, Gwangju, Ulsan, Baengnyeong, Jeju). The timeseries compare observed and simulated monthly mean values averaged at the six sites and error bars indicate the observed minimum and maximum values. The scatterplots compare observed and simulated monthly mean values at all of the six sites.

concentrations of gas phase chemical species, including the hydroxyl radical (OH), formaldehyde (HCHO), AVOCs, and BVOCs.

We find that near-term changes in O_3, NO_2, and SO_2 concentrations in Korea under the SSP1 scenario are −9 %, −42 %, and − 52 %, respectively. Under SSP3, pollutant concentrations change by +1 %, +4 %, and + 22 % in 2045. Long-term changes under the SSP1 scenario are −25 %, −85 %, and − 85 %, respectively, and under SSP3, concentrations change by +9 %, −36 %, and + 7 % in 2095, respectively. We find that noticeable changes in gas phase pollutants are primarily located in urban areas with large anthropogenic sources (Fig. S2).

O_3 change is mainly associated with decreases in precursor concentrations due to strong regulations on anthropogenic emissions under SSP1 (Fig. 4b). However, O_3 is sensitive to increased biogenic emissions in warmer climates and higher CH_4 levels under SSP3 (Fig. 4c). We find that O_3 formation in Korea occurs in a NO_x-limited regime ($VOCs/NO_x > 10$ ppbC/ppbv) in 2095 under SSP1, with significant increases in $VOCs/NO_x$ ratios (Fig. S3) in the regions where O_3 levels decrease. Under SSP3, $VOCs/NO_x$ ratios indicate that most regions in the country will be VOC-limited ($VOCs/NO_x \approx 10$ ppbC/ppbv) in 2095. NO_2 levels decrease in 2095 regardless of scenarios due to changes in primary emissions, but the magnitude of emissions reduction is a factor of three higher in SSP1, resulting in lower surface concentrations by a factor of four than in SSP3. Similarly, SO_2 decreases in 2095 by >50 % compared to the present under SSP1. However, SO_2 increases as SO_2 emissions remain nearly unchanged, and oxidant (OH) levels decrease due to the chemical loss by CH_4 (Fig. 4a and Fig. S3) under SSP3.

Kim et al. (2015) used a coupled chemistry-climate model and simulated an increase in surface O_3 in East Asia in 2050 relative to 2000 under the Representative Concentration Pathway (RCP) 8.5 scenario and O_3 decreases in all other RCP scenarios. The multi-model mean of six CMIP6 models estimated a decrease by ~15 ppbv and an increase by ~6 ppbv in annual O_3 concentrations in East Asia in 2100 relative to the 2005–2014 mean value (Turnock et al., 2020), displaying similar tendencies with our future simulations.

4.2. Aerosol species

Simulated annual mean aerosol concentrations, including $PM_{2.5}$, SIA, and SOA from AVOCs (ASOA) and BVOCs (BSOA), are summarized in Table 3. $PM_{2.5}$ concentrations change by −49 % and + 7 % in 2045 under SSP1 and SSP3, respectively, but eventually decrease by 72 % and 17 % in both scenarios. Simulated results suggest that under the SSP1 scenario, Korea will meet close to the WHO annual mean $PM_{2.5}$ standard of 5 μg m^{-3} in 2095. The relative difference in annual mean concentrations of the chemical components of $PM_{2.5}$ is shown in Fig. 4a.

As most anthropogenic emissions decrease in future scenarios, primary aerosols (BC, POA) and SIA concentrations decrease in the long-term under both SSP1 and SSP3. Future SOA concentrations decrease compared to

Table 3
Simulated annual mean O_3, NO_2, SO_2, $PM_{2.5}$, SIA, and SOA (aromatic and biogenic) concentrations in 2019 and the near-term and long-term future under the SSP1 and SSP3 scenarios. Relative changes ((future − present)/present) are denoted in parentheses.

Species	Present (2019)	SSP1 (2045)	SSP1 (2095)	SSP3 (2045)	SSP3 (2095)
O_3 [ppbv]	44.9	41.0 (−9 %)	33.8 (−25 %)	45.5 (+1 %)	49.0 (+9 %)
NO_2 [ppbv]	12.3	7.1 (−42 %)	1.8 (−85 %)	12.8 (+4 %)	7.9 (−36 %)
SO_2 [ppbv]	2.7	1.3 (−52 %)	0.4 (−85 %)	3.3 (+22 %)	2.9 (+7 %)
$PM_{2.5}$ [μg m^{-3}]	21.7	11.1 (−49 %)	6.1 (−72 %)	23.3 (+7 %)	18.1 (−17 %)
SIA [μg m^{-3}]	14.3	6.9 (−52 %)	1.9 (−87 %)	15.6 (+9 %)	12.5 (−13 %)
ASOA [μg m^{-3}]	2.7	1.6 (−41 %)	0.7 (−74 %)	2.4 (−11 %)	2.1 (−22 %)
BSOA [μg m^{-3}]	1.9	1.6 (−16 %)	1.5 (−21 %)	2.1 (+11 %)	2.3 (+21 %)

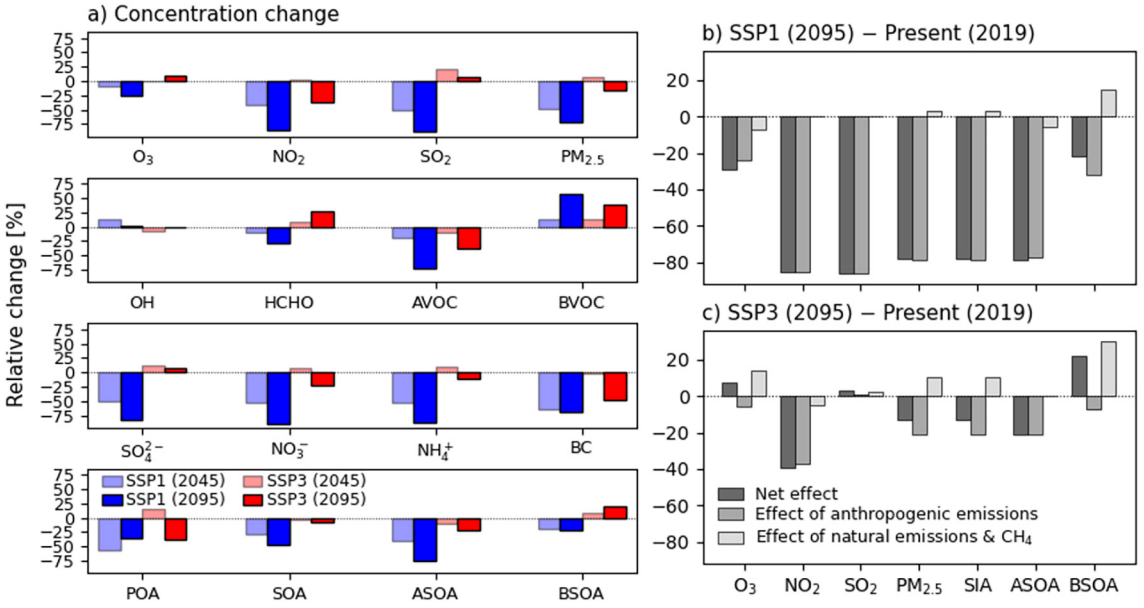

Fig. 4. Comparison of a) present (2019) to future relative changes ((future − present)/present) in simulated gas and aerosol species in Korea, and present to long-term future (2095) relative changes under b) SSP1 and c) SSP3. Each bar in different shades indicates a) changes under each scenario and year, and b − c) the future changes in response to anthropogenic emissions change, natural (biogenic and biomass burning) emissions, and CH_4 level change due to climate change, and the net effect.

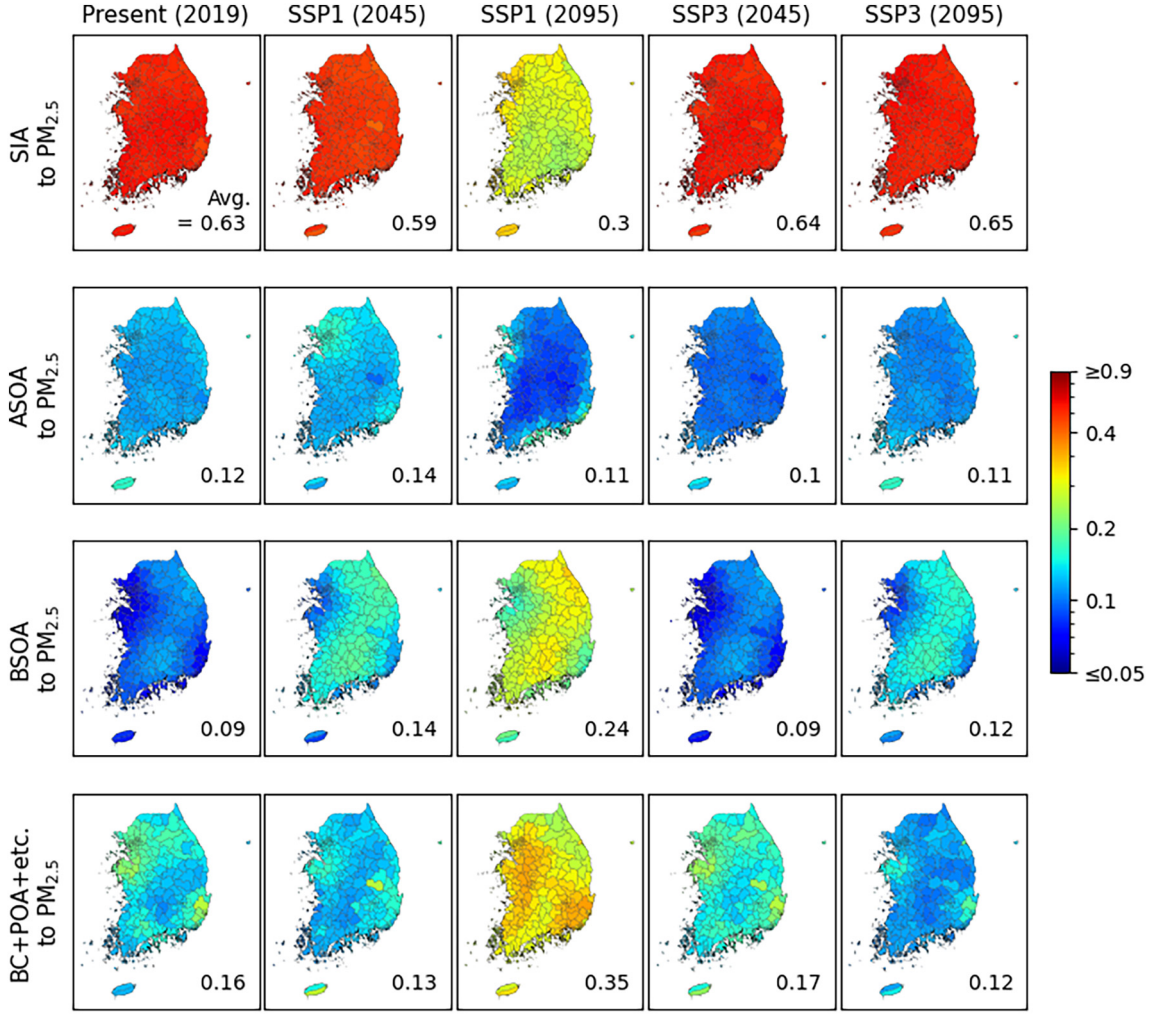

Fig. 5. Simulated annual mean SIA, ASOA, BSOA, and BC + POA + etc. to total $PM_{2.5}$ ratios in the present, near-term, long-term future under SSP1 and SSP3 in Korea. The average values (Avg.) are denoted in the lower-right corners.

present-day levels, but the contribution of BSOA to total $PM_{2.5}$ increases, especially along the middle parts of the country (Fig. 5), where most biogenic sources are located. Figs. 4b – c show that the anthropogenic emissions decrease contributes to the decrease in the major $PM_{2.5}$ components, including SIA, ASOA, and BSOA.

OH, O_3 and NO_3 are the major oxidants that react with BVOCs (isoprene and monoterpenes), and their SOA yields are sensitive to NO_x levels (Pye et al., 2010). Significant reductions in NO_x emissions in 2095 under SSP1 substantially decrease O_3 and NO_3 levels by up to −90 % (Fig. S3), resulting in higher BVOC concentrations compared to 2019. Similar results were reported by Jo et al. (2019), where they found an increase in isoprene under a 50 % decrease in NO_x and SO_2 emissions. Despite the increase in BVOC levels under SSP1, the reduction of NO_x and SO_2 decreases sulfate aerosol levels, increases aerosol pH, and decreases BSOA formation. Our results are consistent with the previous studies (Dong et al., 2022; Jo et al., 2019), which found suppressed aqueous phase formation of BSOA under reduced anthropogenic emissions. We find that the change in BSOA is approximately proportional to the change in SIA concentrations under SSP1. Under SSP3, we find that the effect of increased BVOC emissions and CH_4 levels on BSOA formation is more significant than anthropogenic emissions reduction, resulting in a net increase in BSOA in 2095.

We find that estimated future changes in $PM_{2.5}$ concentrations simulated by a fully-coupled ESM (Sellar et al., 2019) are consistent with the results presented in Table 3. Shim et al. (2020) show that the annual mean $PM_{2.5}$ concentration in East Asia will drop to 10 μg m^{-3} in 2035 and remain at approximately 6 μg m^{-3} between 2081 and 2100 under SSP1. Under SSP3, $PM_{2.5}$ will reach up to 25 μg m^{-3} around 2050 and slowly decrease to 18 μg m^{-3} in 2100. Our results showing a decrease in SOA concentrations by 2.4 and 0.2 μg m^{-3} in 2095 relative to 2019 under SSP1 and SSP3, respectively, are also comparable to the results by Lin et al. (2016), where they estimated an SOA decrease of ~1 μg m^{-3} in Northeast Asia in 2100 relative to 2000 under the RCP8.5 scenario using the Community Earth System Model (CESM).

5. Future changes in premature mortality under the SSPs

Here we present estimated premature mortality attributable to each pollutant using individual RRs, but it should be noted that it is difficult to separate the independent health impact of each pollutant. As people are exposed to a mixture of pollutants in the real atmosphere, the combined effect of unknown chemicals that are co-emitted may be included in our results (Kim et al., 2021).

The cardiovascular and respiratory mortality estimations with 95 % confidence interval RRs due to long-term exposure to O_3, NO_2, SO_2, and $PM_{2.5}$ in Korea based on the AirKorea observations, are estimated to be 10,419 (1271–17,142), 8630 (0–18,713), 3958 (0–9272), and 10,431 (1411–20,643) deaths in 2019 (Fig. 6a). We find that the spatial distribution of O_3-attributable deaths is relatively homogeneous compared to those of NO_2, SO_2, and $PM_{2.5}$, where the majority of deaths are located in the urban and industrial regions. Previous studies in Korea estimated 17,224 (11056–22,772) and 11,924 (11649–12,198) nationwide deaths attributable to $PM_{2.5}$ in 2013 (Kim et al., 2018b) and 2015 (Han et al., 2018), when using RRs from North American cohorts and integrated exposure-response (IER) functions from Burnett et al. (2014). These estimates are higher than our results, as they included lung cancer mortality, which accounted for approximately 20 % of total $PM_{2.5}$-attributable deaths.

The four air pollutants result in 26,034 (1808–48,316) cardiovascular and 7404 (874–17,454) respiratory mortalities (Fig. 6b), and a total of 33,438 (2682–65,770) deaths. We find similar estimates using simulated surface concentrations, sampled coherently in time and space with the observations, with 31,151 (2887–60,265) deaths. Kim et al. (2020) estimated a total of 25,400 (23400–56,600) O_3 and $PM_{2.5}$ attributable to premature mortality in Korea in 2005, comparable to our estimation of 20,850. They estimated a future decrease of 20,000 annual deaths in 2050 under the SSP2 scenario, which assumes moderate socioeconomic growth and lies in between the SSP1 and SSP3 pathways, and 10,100 deaths under the SSP3 scenario. In the following subsections, we discuss estimated future changes in premature mortality under the SSP1 and SSP3 scenarios using our future simulation results.

5.1. Future changes in nationwide total premature mortality

We use future air quality simulations to estimate attributable cardiorespiratory mortality changes using the methodology described in Section 2.2. Fig. 7a compares the nationwide total premature mortality due to O_3, NO_2, SO_2, and $PM_{2.5}$ (≡ SIA + ASOA + BSOA + BC + POA + etc.) exposure under present and future conditions in Korea. As the future population and age structure change differently under each scenario (Fig. S1), this effect is reflected in the estimated mortality as expressed in

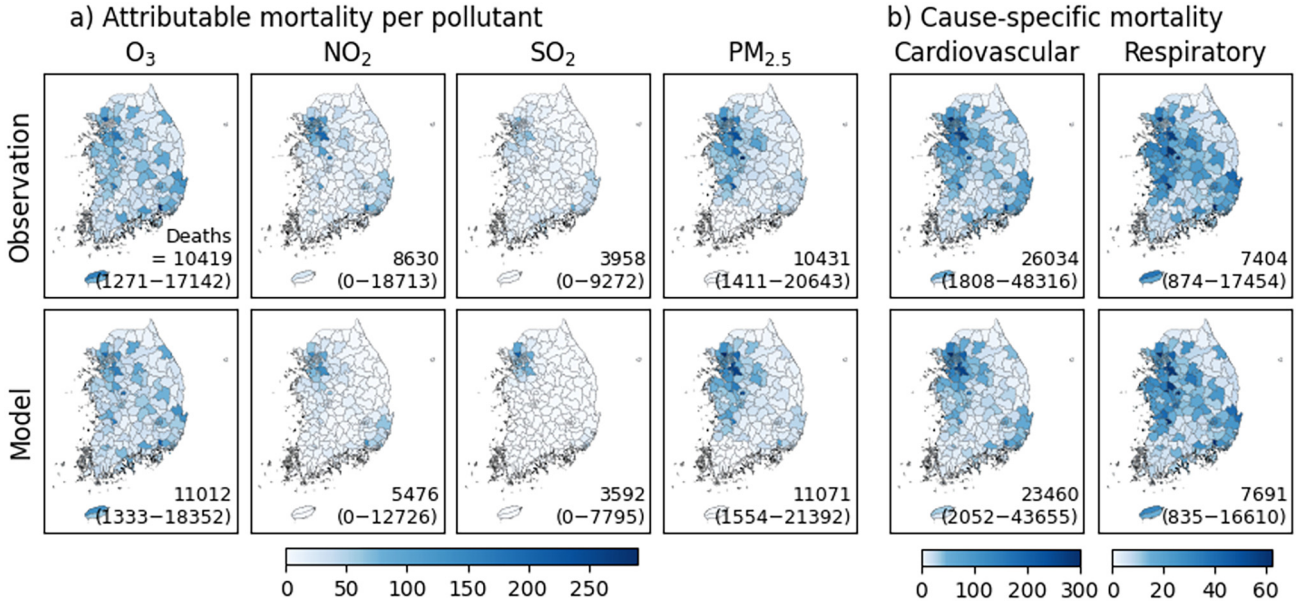

Fig. 6. Spatial distributions of a) O_3, NO_2, SO_2, and $PM_{2.5}$ attributable mortality and b) total attributable cardiovascular and respiratory mortality estimated using observed and simulated surface concentrations, sampled coherently in time and space in Korea during 2019. Total deaths with estimations using 95 % confidence interval RRs in parentheses are denoted in the lower-right corners.

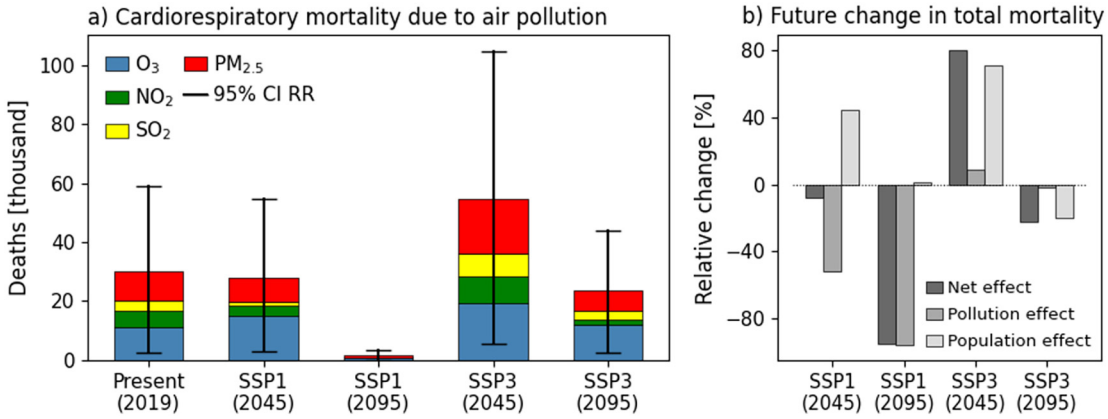

Fig. 7. Estimated a) premature mortality due to O_3, NO_2, SO_2, and $PM_{2.5}$ long-term exposure, and b) present to future relative changes ((future − present)/present) in total premature mortality due to O_3, NO_2, SO_2, and $PM_{2.5}$ under the SSPs in Korea. In panel a), each bar in different shades indicates the mortality attributable to each pollutant, and the error bars indicate estimations of total mortality using 95 % confidence interval RRs. In panel b), each bar in different shades indicates the future changes in response to pollutant concentration change, population and age structure change, and the net effect.

Eq. (2). Fig. 7b quantifies the different effects of pollutant concentration change and population change on future changes in premature mortality.

Estimated total cardiorespiratory excess mortality due to air pollutants shows a slight decrease (−8 %) under SSP1 for the near-term future but eventually decreases by 95 % in 2095. Fig. 7b shows that the effects of pollutant level decrease and population structure change are comparable, but the pollutant effect outweighs the population effect, resulting in a net decrease in premature mortality in the near-term future under SSP1. In the long-term future, a successful reduction in pollutant levels results in a decrease in premature mortality.

Under SSP3, estimated excess mortality increases by 80 % in 2045, and decreases by 22 % in 2095, compared to the present. As the future pollution levels will be similar to or slightly lower than that of the present, the aging population under SSP3 will be the leading cause of increased premature deaths in the near-term future (Fig. S4). Fig. 7b shows that Korea will benefit from improved air quality in the long-term under both the SSP1 and SSP3 scenarios, but the effect of pollutant level decrease greatly differs depending on the future scenario (−96 % versus −2 %).

5.2. Regional changes in future premature mortality

Table 4 compares the present and future premature mortality due to each pollutant estimated using simulated concentrations in each region (Fig. 1) in Korea. As described in Section 2.2 and Table 2, provincial-level baseline mortality rates, municipal-level population data, and region-specific RRs were used to estimate premature mortality. O_3-attributable mortality increases homogeneously (Fig. S5) in all future simulations in general, except for in 2095 under SSP1, where decreases in premature mortality are shown in all regions. Under SSP1, we find that the Northeastern region will benefit most in terms of relative changes (−98 %) in the long-term future O_3-attributable mortality.

Changes in NO_2 and SO_2 attributable mortality in the future are noticeable in the Seoul metropolitan and Southeastern regions. In 2095, NO_2 and SO_2 levels will remain below the concentration-response thresholds of 5.3 and 2 ppbv (Table 2) in all regions under the SSP1 scenario. Under SSP3, NO_2 and SO_2 related mortality will increase in all regions in the near-term future. While NO_2-attributable premature deaths will decrease in all

Table 4
Estimated premature mortality due to O_3, NO_2, SO_2, and $PM_{2.5}$ exposure in each region in Korea in 2019, the near-term, and the long-term future under the SSP1 and SSP3 scenarios. Estimations using 95 % confidence interval RRs are denoted in parentheses.

Species	Region	Present (2019)	SSP1 (2045)	SSP1 (2095)	SSP3 (2045)	SSP3 (2095)
O_3	Seoul metropolitan	3902 (473–6562)	5610 (751–9572)	378 (13–778)	6502 (928–10,806)	4331 (639–6925)
	Central	2074 (249–3422)	2780 (363–4773)	62 (0 − 120)	3796 (566–6185)	2239 (325–3531)
	Southern	1094 (135–1782)	1417 (183–2423)	27 (1–55)	2029 (291–3225)	1126 (164–1770)
	Southeastern	3486 (413–5774)	4296 (572–7461)	156 (5–320)	5968 (862–9834)	3632 (524–5816)
	Northeastern	537 (62–901)	731 (90–1250)	10 (0–19)	1020 (155–1625)	544 (78–867)
	Total	11,093 (1332–18,441)	14,834 (1959–25,479)	633 (19–1292)	19,315 (2802–31,675)	11,872 (1730–18,909)
NO_2	Seoul metropolitan	3162 (0–7015)	2468 (0–6076)	0 (0–0)	5096 (0–11,483)	1308 (0–3252)
	Central	639 (0–1674)	277 (0–777)	0 (0–0)	1172 (0–3007)	144 (0–403)
	Southern	141 (0–378)	34 (0–108)	0 (0–0)	290 (0–766)	25 (0–66)
	Southeastern	1434 (0–3445)	744 (0–1927)	0 (0–0)	2561 (0–6070)	423 (0, −1074)
	Northeastern	84 (0 − 213)	30 (0–80)	0 (0–0)	160 (0–399)	16 (0–46)
	Total	5460 (0–12,725)	3553 (0–8968)	0 (0–0)	9279 (0–21,725)	1916 (0–4841)
SO_2	Seoul metropolitan	3073 (0–6561)	1429 (0–3449)	0 (0–0)	6462 (0–13,247)	2676 (0–5665)
	Central	31 (0–94)	0 (0–0)	0 (0–0)	143 (0–383)	38 (0–99)
	Southern	7 (0–18)	0 (0–0)	0 (0–0)	23 (0–56)	8 (0–19)
	Southeastern	454 (0–1063)	0 (0–0)	0 (0–0)	1076 (0–2478)	389 (0–930)
	Northeastern	4 (0–9)	0 (0–0)	0 (0–0)	41 (0 − 102)	5 (0 − 12)
	Total	3569 (0–7745)	1429 (0–3449)	0 (0–0)	7745 (0–16,266)	3116 (0–6725)
$PM_{2.5}$	Seoul metropolitan	6067 (977–9859)	5063 (703–9150)	704 (81–1440)	10,472 (1733–16,738)	4033 (600–6746)
	Central	2520 (420–4217)	1841 (282–3468)	200 (20–422)	4635 (810–7590)	1655 (265–2903)
	Southern	0 (0–1290)	0 (0–827)	0 (0–40)	0 (0–2460)	0 (0–848)
	Southeastern	1311 (0–3565)	910 (0–2520)	73 (0–280)	2619 (0–6553)	841 (0–2266)
	Northeastern	263 (0–1014)	196 (0–883)	15 (0–85)	543 (0–1876)	189 (0–744)
	Total	10,161 (1397–19,945)	8010 (985–16,848)	992 (101–2267)	18,269 (2543–35,217)	6718 (865–13,507)

regions in the long-term future, the Seoul metropolitan area and Southeastern regions will be the only regions experiencing a decrease in SO_2-attributable premature deaths in 2095.

$PM_{2.5}$-attributable mortality generally decreases in all future simulations except for 2045 under SSP3, where the mortality doubles in the Southeastern and Northeastern regions compared to the present. While the Southern region showed the lowest simulated annual mean $PM_{2.5}$ of 18.4 μg m^{-3} in 2019, Byun et al. (2021) found weak associations between PM and cardiorespiratory mortality (RR < 1), which resulted in no excess deaths due to $PM_{2.5}$ in this region. The Seoul metropolitan area shows the highest $PM_{2.5}$ levels (7.7 and 24.0 μg m^{-3} under SSP1 and SSP3, respectively) among the five regions in 2095. Although the number of deaths avoided from future $PM_{2.5}$ air quality improvement is the largest in this region, the relative changes are the largest in the eastern areas (Southeast and Northeast).

The long-term health burden of chemical components comprising $PM_{2.5}$ may differ, but it is difficult to quantify due to the lack of long-term observations. Therefore, most epidemiologic studies estimated the association between total PM mass and premature mortality in Korea (Byun et al., 2021). While Pye et al. (2021) found significant associations between SOA and cardiorespiratory mortality in the US, Nault et al. (2021) and Ridley et al. (2017) estimated the potential health impacts of ASOA and OA using CTM simulations by multiplying the mass fraction of the component to $PM_{2.5}$ to the estimated $PM_{2.5}$-attributable mortality. In a similar matter, as the relative abundance of simulated BSOA among the major components increases by at least a factor of ~2.5 in 2095 under SSP1 (Fig. 5), especially in the Northeastern region, this emphasizes the potential health burden of BSOA on a local scale in the future. Under SSP3, SIA comprises more than half of the total $PM_{2.5}$ mass, with a relatively homogeneous spatial distribution.

6. Conclusions

We analyzed near-term (2045) and long-term (2095) future changes in O_3, NO_2, SO_2, and $PM_{2.5}$ concentrations and their cardiorespiratory health burden relative to the present (2019) in Korea by using the GEOS-Chem 3-D CTM and CRFs based on Korean cohorts and health surveys. We considered future changes in anthropogenic and natural emissions under SSP1 and SSP3 based on CMIP6 experiments, and the future population and age structures in Korea from the SSP database.

Significant reductions in precursor emissions under the SSP1 scenario will decrease future concentrations of most gas and aerosol species compared to the present. The improvement in air quality will eventually lead to a large decrease (−94 %) in premature mortality in 2095. Despite the decrease in premature mortality, the relative abundance of BSOA among the major components of $PM_{2.5}$ emphasizes the need to consider BSOA and its health impact on a local scale in the future.

Under the SSP3 scenario, O_3 will increase in the future, mainly driven by increased biogenic emissions under the warming climate. Concentrations of NO_2, SO_2, SIA, POA, and ASOA generally follow the trends in anthropogenic emissions change. In the long-term future, overall pollutant concentrations will be similar to or slightly lower than that of the present, with decreases in NO_2 and $PM_{2.5}$ and increases in O_3 and SO_2. The aging population under SSP3 will cause increased premature deaths in the near future, but an overall decrease in the total adult population will decrease (−3 %) in premature mortality in 2095.

A few assumptions and uncertainties serve as limitations of this study. First, as we fixed the meteorological fields to those of 2019, we cannot quantify the meteorological impact of climate change on air quality and the chemistry-climate feedback of air pollutants (Kim et al., 2015). Kim et al. (2020) considered both the emissions control and the change in radiative forcing under the SSP scenarios and simulated a decrease in O_3 levels and an increase in $PM_{2.5}$ in 2050 relative to 2005 under the SSP3 scenario, and estimated a 40 % decrease in premature deaths in Korea. These results are contrary to our results which showed increased O_3 and $PM_{2.5}$ levels in 2045 relative to 2019. As the anthropogenic emissions in 2005 were ~ 10 % lower than those in 2019 (https://www.air.go.kr/eng/aps/emission/year.do?menuId = 98), it is difficult for an apples-to-apples comparison. However, Kim et al. (2020) shows that the future health burden benefit (−40 %) is the net effect of a 3 % increase due to emissions control, and a 43 % decrease due to climate mitigation by stabilizing the radiative forcing level at 3.4 W m^{-2}. Therefore, a fully coupled chemistry-climate model would be required for further analysis.

Second, we applied the RR estimated for PM_{10} to calculate premature mortality attributable to $PM_{2.5}$. However, $PM_{2.5}$ is more likely to reach deeper into the circulatory or respiratory system (Oberdörster et al., 2005) with larger toxicity than PM_{10} (Kelly and Fussell, 2012), which may imply a larger RR for $PM_{2.5}$ (Yorifuji et al., 2015). Also, we presented estimated premature mortality attributable to each pollutant using individual RRs, but exposure to a mixture of pollutants that are co-emitted can simultaneously affect the human cardiovascular and respiratory system (Kim et al., 2021). Therefore, uncertainties should be noted when interpreting the estimated health impact of each pollutant. Nonetheless, as the first study to use area-specific CRFs based on Korean cohorts and municipal-level mortality rates to estimate future mortality changes in Korea, our results imply a substantial difference in the long-term health outcomes in Korea depending on the future emission and population scenario and provide insight into the efficacy of future regulation policies.

CRediT authorship contribution statement

Yujin J. Oak: Conceptualization, Investigation, Writing – original draft, Visualization. **Rokjin J. Park:** Conceptualization, Writing – review & editing. **Jong-Tae Lee:** Resources. **Garam Byun:** Resources.

Data availability

Data will be made available on request.

Declaration of competing interest

The authors declare that they have no known competing financial interests or personal relationships that could have appeared to influence the work reported in this paper.

Acknowledgements

This study was supported by the National Research Foundation of Korea (NRF) grant funded by the Korean Ministry of Science and ICT (MSIT) (NRF-2018R1A2B300449415, NRF-2021M3I6A108680712).

Appendix A. Supplementary data

Supplementary data to this article can be found online at https://doi.org/10.1016/j.scitotenv.2022.161134.

References

Amann, M., Derwent, D., Forsberg, B., Hänninen, O., Hurley, F., Krzyzanowski, M., de Leeuw, F., Liu, S.J., Mandin, C., Schneider, J., Schwarze, P., Simpson, D., 2008. Health Risks of Ozone From Long-range Transboundary Air Pollution. World Health Organization. Regional Office for Europe, Copenhagen PP - Copenhagen.

Anenberg, S.C., Horowitz, L.W., Tong, D.Q., West, J.J., 2010. An estimate of the global burden of anthropogenic ozone and fine particulate matter on premature human mortality using atmospheric modeling. Environ. Health Perspect. 118, 1189–1195. https://doi.org/10.1289/ehp.0901220.

Bae, S., Kwon, H.J., 2019. Current state of research on the risk of morbidity and mortality associated with air pollution in Korea. YonseiMed. J. https://doi.org/10.3349/ymj.2019.60.3.243.

Burnett, R., Pope, C., Ezzati, M., Olives, C., Lim, S., Mehta, S., Shin, H., Singh, G., Hubbell, B., Brauer, M., Anderson, H., Smith, K., Balmes, J., Bruce, N., Kan, H., Laden, F., Prüss-Ustün, A., Turner, M., Gapstur, S., Cohen, A., 2014. An integrated risk function for estimating the global burden of disease attributable to ambient fine particulate matter exposure. Environ. Health Perspect. 122. https://doi.org/10.1289/ehp.1307049.

Byun, G., Choi, Y., Gil, J., Cha, J., Lee, M., Lee, J.-T., 2021. Health and economic burden attributable to particulate matter in South Korea: considering spatial variation in relative risk. J. Environ. HealthSci. 47, 486–495. https://doi.org/10.5668/JEHS.2021.47.5.486.

Byun, G., Choi, Y., Kim, S., Lee, J.-T., 2022. Long-term exposure to ambient ozone and mortality in a population-based cohort of South Korea: considering for an alternative exposure time metric. Environ. Pollut. 314, 120300. https://doi.org/10.1016/j.envpol.2022.120300.

Cao, Y., Yue, X., Liao, H., Yang, Y., Zhu, J., Chen, L., Tian, C., Lei, Y., Zhou, H., Ma, Y., 2021. Ensemble projection of global isoprene emissions by the end of 21st century using CMIP6 models. Atmos. Environ. 267, 118766. https://doi.org/10.1016/j.atmosenv.2021.118766.

Chen, J., Hoek, G., 2020. Long-term exposure to PM and all-cause and cause-specific mortality: a systematic review and meta-analysis. Environ. Int. 143, 105974. https://doi.org/10.1016/j.envint.2020.105974.

Choi, J., Park, R.J., Lee, H.-M., Lee, S., Jo, D.S., Jeong, J.I., Henze, D.K., Woo, J.-H., Ban, S.-J., Lee, M.-D., Lim, C.-S., Park, M.-K., Shin, H.J., Cho, S., Peterson, D., Song, C.-K., 2019. Impacts of local vs. trans-boundary emissions from different sectors on PM2.5 exposure in South Korea during the KORUS-AQ campaign. Atmos. Environ. 203, 196–205. https://doi.org/10.1016/j.atmosenv.2019.02.008.

Chong, H., Lee, S., Kim, J., Jeong, U., Li, C., Krotkov, N., Nowlan, C., Al-Saadi, J., Janz, S., Kowalewski, M., Ahn, M.-H., Kang, M., Joanna, J., Haffner, D., Hu, L., Castellanos, P., Huey, L., Choi, M., Song, C., Koo, J.-H., 2020. High-resolution mapping of SO2 using airborne observations from the GeoTASO instrument during the KORUS-AQ field study: PCA-based vertical column retrievals. Remote Sens. Environ. 241, 111725. https://doi.org/10.1016/j.rse.2020.111725.

Chowdhury, S., Dey, S., Smith, K.R., 2018. Ambient PM2.5 exposure and expected premature mortality to 2100 in India under climate change scenarios. Nat. Commun. 9. https://doi.org/10.1038/s41467-017-02755-y.

Crouse, D.L., Peters, P.A., Hystad, P., Brook, J.R., van Donkelaar, A., Martin, R.V., Villeneuve, P.J., Jerrett, M., Goldberg, M.S., Arden Pope, C., Brauer, M., Brook, R.D., Robichaud, A., Menard, R., Burnett, R.T., 2015. Ambient PM2.5, O3, and NO2 exposures and associations with mortality over 16 years of follow-up in the Canadian census health and environment cohort (CanCHEC). Environ. Health Perspect. 123, 1180–1186. https://doi.org/10.1289/ehp.1409276.

Darmenov, A., da Silva, A., 2015. The Quick Fire Emissions Dataset (QFED) – Documentation of Versions 2.1, 2.2 and 2.4.

Dong, X., Liu, Yaman, Li, X., Yue, M., Liu, Yawen, Ma, Z., Zheng, H., Huang, R., Wang, M., 2022. Modeling analysis of biogenic secondary organic aerosol dependence on anthropogenic emissions in China. Environ. Sci. Technol. Lett. 9, 286–292. https://doi.org/10.1021/acs.estlett.2c00104.

Dunlea, E.J., Herndon, S.C., Nelson, D.D., Volkamer, R.M., San Martini, F., Sheehy, P.M., Zahniser, M.S., Shorter, J.H., Wormhoudt, J.C., Lamb, B.K., Allwine, E.J., Gaffney, J.S., Marley, N.A., Grutter, M., Marquez, C., Blanco, S., Cardenas, B., Retama, A., Ramos Villegas, C.R., Kolb, C.E., Molina, L.T., Molina, M.J., 2007. Evaluation of nitrogen dioxide chemiluminescence monitors in a polluted urban environment. Atmos. Chem. Phys. 7, 2691–2704. https://doi.org/10.5194/acp-7-2691-2007.

Fann, N., Nolte, C., Dolwick, P., Spero, T., Brown, A., Phillips, S., Anenberg, S., 2014. The geographic distribution and economic value of climate change-related ozone health impacts in the United States in 2030. J. Air Waste Manag. Assoc. 65. https://doi.org/10.1080/10962247.2014.996270.

Faustini, A., Rapp, R., Forastiere, F., 2014. Nitrogen dioxide and mortality: review and meta-analysis of long-term studies. Eur. Respir. J. https://doi.org/10.1183/09031936.00114713.

Fountoukis, C., Nenes, A., 2007. ISORROPIA II: a computationally efficient thermodynamic equilibrium model for K+–Ca2+–Mg2+–NH4+–Na+–SO42−–NO3<sup/>. Atmos. Chem. Phys. 7, 4639–4659. https://doi.org/10.5194/acp-7-4639-2007.

Gidden, M.J., Riahi, K., Smith, S.J., Fujimori, S., Luderer, G., Kriegler, E., van Vuuren, D.P., van den Berg, M., Feng, L., Klein, D., Calvin, K., Doelman, J.C., Frank, S., Fricko, O., Harmsen, M., Hasegawa, T., Havlik, P., Hilaire, J., Hoesly, R., Horing, J., Popp, A., Stehfest, E., Takahashi, K., 2019. Global emissions pathways under different socioeconomic scenarios for use in CMIP6: a dataset of harmonized emissions trajectories through the end of the century. Geosci. Model Dev. 12, 1443–1475. https://doi.org/10.5194/gmd-12-1443-2019.

Guenther, A.B., Jiang, X., Heald, C.L., Sakulyanontvittaya, T., Duhl, T., Emmons, L.K., Wang, X., 2012. The model of emissions of gases and aerosols from nature version 2.1 (MEGAN2.1): an extended and updated framework for modeling biogenic emissions. Geosci. Model Dev. 5, 1471–1492. https://doi.org/10.5194/gmd-5-1471-2012.

Han, C., Kim, S., Lim, Y.-H., Bae, H.-J., Hong, Y.-C., 2018. Spatial and temporal trends of number of deaths attributable to ambient PM2.5 in the Korea. J. Korean Med. Sci. 33.

Hodzic, A., Kasibhatla, P.S., Jo, D.S., Cappa, C.D., Jimenez, J.L., Madronich, S., Park, R.J., 2016. Rethinking the global secondary organic aerosol (SOA) budget: stronger production, faster removal, shorter lifetime. Atmos. Chem. Phys. 16, 7917–7941. https://doi.org/10.5194/acp-16-7917-2016.

Hoek, G., Krishnan, R.M., Beelen, R., Peters, A., Ostro, B., Brunekreef, B., Kaufman, J.D., 2013. Long-term air pollution exposure and cardio-respiratory mortality: a review. Environ. Health Glob. Access Sci. Source https://doi.org/10.1186/1476-069X-12-43.

Huangfu, P., Atkinson, R., 2020. Long-term exposure to NO2 and O3 and all-cause and respiratory mortality: a systematic review and meta-analysis. Environ. Int. https://doi.org/10.1016/j.envint.2020.105998.

Hwang, J., Kwon, J., Yi, H., Bae, H.-J., Jang, M., Kim, N., 2020. Association between long-term exposure to air pollutants and cardiopulmonary mortality rates in South Korea. BMC Public Health 20, 1402. https://doi.org/10.1186/s12889-020-09521-8.

Jathar, S.H., Gordon, T.D., Hennigan, C.J., Pye, H.O., Pouliot, G., Adams, P.J., Donahue, N.M., Robinson, A.L., 2014. Unspeciated organic emissions from combustion sources and their influence on the secondary organic aerosol budget in the United States. Proc. Natl. Acad. Sci. U. S. A. 111, 10473–10478. https://doi.org/10.1073/pnas.1323740111.

Jerrett, M., Burnett, R.T., Pope, C.A., Ito, K., Thurston, G., Krewski, D., Shi, Y., Calle, E., Thun, M., 2009. Long-term ozone exposure and mortality. N. Engl. J. Med. 360, 1085–1095. https://doi.org/10.1056/nejmoa0803894.

Jo, D.S., Park, R.J., Kim, M.J., Spracklen, D.V., 2013. Effects of chemical aging on global secondary organic aerosol using the volatility basis set approach. Atmos. Environ. 81, 230–244. https://doi.org/10.1016/j.atmosenv.2013.08.055.

Jo, D.S., Hodzic, A., Emmons, L.K., Marais, E.A., Peng, Z., Nault, B.A., Hu, W., Campuzano-Jost, P., Jimenez, J.L., 2019. A simplified parameterization of isoprene-epoxydiol-derived secondary organic aerosol (IEPOX-SOA) for global chemistry and climate models: a case study with GEOS-Chem v11–02-rc. Geosci. Model Dev. 12, 2983–3000. https://doi.org/10.5194/gmd-12-2983-2019.

KC, S., Lutz, W., 2017. The human core of the shared socioeconomic pathways: population scenarios by age, sex and level of education for all countries to 2100. Glob. Environ. Chang. 42, 181–192. https://doi.org/10.1016/j.gloenvcha.2014.06.004.

Kelly, F.J., Fussell, J.C., 2012. Size, source and chemical composition as determinants of toxicity attributable to ambient particulate matter. Atmos. Environ. 60, 504–526. https://doi.org/10.1016/j.atmosenv.2012.06.039.

Kim, H., Zhang, Q., Bae, G.N., Kim, J.Y., Lee, S.B., 2017. Sources and atmospheric processing of winter aerosols in Seoul, Korea: insights from real-time measurements using a high-resolution aerosol mass spectrometer. Atmos. Chem. Phys. 17, 2009–2033. https://doi.org/10.5194/acp-17-2009-2017.

Kim, H., Zhang, Q., Heo, J., 2018. Influence of intense secondary aerosol formation and long-range transport on aerosol chemistry and properties in the Seoul metropolitan area during spring time: results from KORUS-AQ. Atmos. Chem. Phys. 18, 7149–7168. https://doi.org/10.5194/acp-18-7149-2018.

Kim, H., Kim, Hyomi, Lee, J.-T., 2019. Spatial variation in lag structure in the short-term effects of air pollution on mortality in seven major South Korean cities, 2006–2013. Environ. Int. 125, 595–605. https://doi.org/10.1016/j.envint.2018.09.004.

Kim, H., Byun, G., Choi, Y., Kim, S., Kim, S.Y., Lee, J.T., 2021. Effects of long-term exposure to air pollution on all-cause mortality and cause-specific mortality in seven major cities of South Korea: korean national health and nutritional examination surveys with mortality follow-up. Environ. Res. 192. https://doi.org/10.1016/j.envres.2020.110290.

Kim, J.-H., Oh, I.-H., Park, J.-H., Cheong, H.-K., 2018. Premature deaths attributable to long-term exposure to ambient fine particulate matter in the Republic of Korea. J. Korean Med. Sci. 33.

Kim, M.J., Park, R.J., Ho, C.-H., Woo, J.-H., Choi, K.-C., Song, C.-K., Lee, J.-B., 2015. Future ozone and oxidants change under the RCP scenarios. Atmos. Environ. 101, 103–115. https://doi.org/10.1016/j.atmosenv.2014.11.016.

Kim, S., Kim, H., Lee, J.-T., 2019. Interactions between ambient air particles and greenness on cause-specific mortality in seven Korean metropolitan cities, 2008–2016. Int. J. Environ. Res. Public Health 16, 1866. https://doi.org/10.3390/ijerph16101866.

Kim, S.E., Xie, Y., Dai, H., Fujimori, S., Hijioka, Y., Honda, Y., Hashizume, M., Masui, T., Hasegawa, T., Xu, X., Yi, K., Kim, H., 2020. Air quality co-benefits from climate mitigation for human health in South Korea. Environ. Int. 136. https://doi.org/10.1016/j.envint.2020.105507.

Lee, S., Park, R.J., Hong, S.Y., Koo, M.S., Jeong, J.I., Yeh, S.W., Son, S.W., 2022. A new chemistry-climate model GRIMs-CCM: model evaluation of interactive chemistry-meteorology simulations. Asia-Pac.J. Atmos. Sci. 2. https://doi.org/10.1007/s13143-022-00281-6.

Lin, G., Penner, J., Zhou, C., 2016. How will SOA change in the future? Geophys.Res. Lett. 43. https://doi.org/10.1002/2015GL067137 n/a-n/a.

Luo, G., Yu, F., Moch, J.M., 2020. Further improvement of wet process treatments in GEOS-Chem v12.6.0: impact on global distributions of aerosols and aerosol precursors. Geosci. Model Dev. 13, 2879–2903. https://doi.org/10.5194/gmd-13-2879-2020.

Marais, E.A., Jacob, D.J., Jimenez, J.L., Campuzano-Jost, P., Day, D.A., Hu, W., Krechmer, J., Zhu, L., Kim, P.S., Miller, C.C., Fisher, J.A., Travis, K., Yu, K., Hanisco, T.F., Wolfe, G.M., Arkinson, H.L., Pye, H.O.T., Froyd, K.D., Liao, J., McNeill, V.F., 2016. Aqueous-phase mechanism for secondary organic aerosol formation from isoprene: application to the southeast United States and co-benefit of SO2 emission controls. Atmos. Chem. Phys. 16, 1603–1618. https://doi.org/10.5194/acp-16-1603-2016.

McDuffie, E., Smith, S., O'Rourke, P., Tibrewal, K., Venkataraman, C., Marais, E., Zheng, B., Crippa, M., Brauer, M., Martin, R., 2020. A global anthropogenic emission inventory of atmospheric pollutants from sector-and fuel-specific sources (1970-2017): an application of the Community Emissions Data System (CEDS). Earth Syst. Sci. Data Discuss. https://doi.org/10.5194/essd-2020-103.

Nault, B.A., Jo, D.S., McDonald, B.C., Campuzano-Jost, P., Day, D.A., Hu, W., Schroder, J.C., Allan, J., Blake, D.R., Canagaratna, M.R., Coe, H., Coggon, M.M., DeCarlo, P.F., Diskin, G.S., Dunmore, R., Flocke, F., Fried, A., Gilman, J.B., Gkatzelis, G., Hamilton, J.F., Hanisco, T.F., Hayes, P.L., Henze, D.K., Hodzic, A., Hopkins, J., Hu, M., Huey, L.G., Jobson, B.T., Kuster, W.C., Lewis, A., Li, M., Liao, J., Nawaz, M.O., Pollack, I.B., Peischl, J., Rappenglück, B., Reeves, C.E., Richter, D., Roberts, J.M., Ryerson, T.B., Shao, M., Sommers, J.M., Walega, J., Warneke, C., Weibring, P., Wolfe, G.M., Young, D.E., Yuan, B., Zhang, Q., de Gouw, J.A., Jimenez, J.L., 2021. Secondary organic aerosols from anthropogenic volatile organic compounds contribute substantially to air pollution mortality. Atmos. Chem. Phys. 21, 11201–11224. https://doi.org/10.5194/acp-21-11201-2021.

Oak, Y.J., Park, R.J., Schroeder, J.R., Crawford, J.H., Blake, D.R., Weinheimer, A.J., Woo, J.-H., Kim, S.-W., Yeo, H., Fried, A., Wisthaler, A., Brune, W.H., 2019. Evaluation of simulated O3 production efficiency during the KORUS-AQ campaign: implications for anthropogenic NOx emissions in Korea. Elementa 7. https://doi.org/10.1525/elementa.394.

Oak, Y.J., Park, R.J., Jo, D.S., Hodzic, A., Jimenez, J.L., Campuzano-Jost, P., Nault, B.A., Kim, H., Kim, H., Ha, E.S., Song, C.-K., Yi, S.-M., Diskin, G.S., Weinheimer, A.J., Blake, D.R., Wisthaler, A., Shim, M., Shin, Y., 2022. Evaluation of secondary organic aerosol (SOA)

simulations for Seoul,Korea. J. Adv. Model. Earth Syst. 14. https://doi.org/10.1029/2021MS002760.

Oberdörster, G., Oberdörster, E., Oberdörster, J., 2005. Nanotoxicology: an emerging discipline evolving from studies of ultrafine particles. Environ. Health Perspect. 113, 823–839. https://doi.org/10.1289/ehp.7339.

Orru, H., Andersson, C., Ebi, K.L., Langner, J., Åström, C., Forsberg, B., 2012. Impact of climate change on ozone related mortality and morbidity in Europe. Eur. Respir. J. https://doi.org/10.1183/09031936.00210411 erj02104-2011.

Pai, S.J., Heald, C.L., Pierce, J.R., Farina, S.C., Marais, E.A., Jimenez, J.L., Campuzano-Jost, P., Nault, B.A., Middlebrook, A.M., Coe, H., Shilling, J.E., Bahreini, R., Dingle, J.H., Vu, K., 2019. An evaluation of global organic aerosol schemes using airborne observations. Atmos. Chem. Phys. Discuss. 2019, 1–39. https://doi.org/10.5194/acp-2019-331.

Park, R.J., Jacob, D.J., Chin, M., Martin, R.V., 2003. Sources of carbonaceous aerosols over the United States and implications for natural visibility. J. Geophys. Res. Atmos. 108. https://doi.org/10.1029/2002jd003190.

Park, R.J., Jacob, D.J., Field, B.D., Yantosca, R.M., Chin, M., 2004. Natural and transboundary pollution influences on sulfate-nitrate-ammonium aerosols in the United States: implications for policy. J. Geophys. Res. Atmos. 109. https://doi.org/10.1029/2003JD004473.

Park, R.J., Oak, Y.J., Emmons, L.K., Kim, C.-H., Pfister, G.G., Carmichael, G.R., Saide, P.E., Cho, S.-Y., Kim, S., Woo, J.-H., Crawford, J.H., Gaubert, B., Lee, H.-J., Park, S.-Y., Jo, Y.-J., Gao, M., Tang, B., Stanier, C.O., Shin, S.S., Park, H.Y., Bae, C., Kim, E., 2021. Multi-model intercomparisons of air quality simulations for the KORUS-AQ campaign. Elem. Sci. Anthr. 9. https://doi.org/10.1525/elementa.2021.00139.

Park, S., Allen, R., Lim, C.-H., 2020. A likely increase in fine particulate matter and premature mortality under future climate change. Air Qual. Atmos. Health 13. https://doi.org/10.1007/s11869-019-00785-7.

Philip, S., Martin, R., Pierce, J., Jimenez, J.L., Zhang, Q., Spracklen, D., Nowlan, C., Lamsal, L., Cooper, M., Krotkov, N., 2014. Spatially and seasonally resolved estimate of the ratio of organic mass to organic carbon. Atmos. Environ. 87, 34–40. https://doi.org/10.1016/j.atmosenv.2013.11.065.

Pye, H.O.T., Chan, A.W.H., Barkley, M.P., Seinfeld, J.H., 2010. Global modeling of organic aerosol: the importance of reactive nitrogen (NOx and NO3). Atmos. Chem. Phys. 10, 11261–11276. https://doi.org/10.5194/acp-10-11261-2010.

Pye, H.O.T., Ward-Caviness, C.K., Murphy, B.N., Appel, K.W., Seltzer, K.M., 2021. Secondary organic aerosol association with cardiorespiratory disease mortality in the United States. Nat. Commun. 12, 7215. https://doi.org/10.1038/s41467-021-27484-1.

Reed, C., Evans, M.J., Di Carlo, P., Lee, J.D., Carpenter, L.J., 2016. Interferences in photolytic NO2 measurements: explanation for an apparent missing oxidant? Atmos. Chem. Phys. 16, 4707–4724. https://doi.org/10.5194/acp-16-4707-2016.

Ridley, D.A., Heald, C.L., Ridley, K.J., Kroll, J.H., 2017. Causes and consequences of decreasing atmospheric organic aerosol in the United States. Proc. Natl. Acad. Sci. U. S. A. 115, 290–295. https://doi.org/10.1073/pnas.1700387115.

Saunois, M., Stavert, A.R., Poulter, B., Bousquet, P., Canadell, J.G., Jackson, R.B., Raymond, P.A., Dlugokencky, E.J., Houweling, S., Patra, P.K., Ciais, P., Arora, V.K., Bastviken, D., Bergamaschi, P., Blake, D.R., Brailsford, G., Bruhwiler, L., Carlson, K.M., Carrol, M., Castaldi, S., Chandra, N., Crevoisier, C., Crill, P.M., Covey, K., Curry, C.L., Etiope, G., Frankenberg, C., Gedney, N., Hegglin, M.I., Höglund-Isaksson, L., Hugelius, G., Ishizawa, M., Ito, A., Janssens-Maenhout, G., Jensen, K.M., Joos, F., Kleinen, T., Krummel, P.B., Langenfelds, R.L., Laruelle, G.G., Liu, L., Machida, T., Maksyutov, S., McDonald, K.C., McNorton, J., Miller, P.A., Melton, J.R., Morino, I., Müller, J., Murguia-Flores, F., Naik, V., Niwa, Y., Noce, S., O'Doherty, S., Parker, R.J., Peng, C., Peng, S., Peters, G.P., Prigent, C., Prinn, R., Ramonet, M., Regnier, P., Riley, W.J., Rosentreter, J.A., Segers, A., Simpson, I.J., Shi, H., Smith, S.J., Steele, L.P., Thornton, B.F., Tian, H., Tohjima, Y., Tubiello, F.N., Tsuruta, A., Viovy, N., Voulgarakis, A., Weber, T.S., van Weele, M., van der Werf, G.R., Weiss, R.F., Worthy, D., Wunch, D., Yin, Y., Yoshida, Y., Zhang, W., Zhang, Z., Zhao, Y., Zheng, B., Zhu, Q., Zhu, Q., Zhuang, Q., 2020. The global methane budget 2000–2017. Earth Syst. Sci. Data 12, 1561–1623. https://doi.org/10.5194/essd-12-1561-2020.

Sellar, A.A., Jones, C.G., Mulcahy, J.P., Tang, Y., Yool, A., Wiltshire, A., O'Connor, F.M., Stringer, M., Hill, R., Palmieri, J., Woodward, S., de Mora, L., Kuhlbrodt, T., Rumbold, S.T., Kelley, D.I., Ellis, R., Johnson, C.E., Walton, J., Abraham, N.L., Andrews, M.B., Andrews, T., Archibald, A.T., Berthou, S., Burke, E., Blockley, E., Carslaw, K., Dalvi, M., Edwards, J., Folberth, G.A., Gedney, N., Griffiths, P.T., Harper, A.B., Hendry, M.A., Hewitt, A.J., Johnson, B., Jones, A., Jones, C.D., Keeble, J., Liddicoat, S., Morgenstern, O., Parker, R.J., Predoi, V., Robertson, E., Siahaan, A., Smith, R.S., Swaminathan, R., Woodhouse, M.T., Zeng, G., Zerroukat, M., 2019. UKESM1: description and evaluation of the U.K. Earth system model. J. Adv. Model. Earth Syst. 11, 4513–4558. https://doi.org/10.1029/2019MS001739.

Shim, S., Seo, J., Kwon, S.H., Lee, J.H., Sung, H.M., Boo, K.O., Byun, Y.H., Lim, Y.J., Kim, Y.H., 2020. Impact of future air quality in East Asia under SSP scenarios. Atmosphere-Korea 30, 439–454.

Silva, R.A., West, J.J., Lamarque, J.F., Shindell, D.T., Collins, W.J., Dalsoren, S., Faluvegi, G., Folberth, G., Horowitz, L.W., Nagashima, T., Naik, V., Rumbold, S.T., Sudo, K., Takemura, T., Bergmann, D., Cameron-Smith, P., Cionni, I., Doherty, R.M., Eyring, V., Josse, B., MacKenzie, I.A., Plummer, D., Righi, M., Stevenson, D.S., Strode, S., Szopa, S., Zengast, G., 2016. The effect of future ambient air pollution on human premature mortality to 2100 using output from the ACCMIP model ensemble. Atmos. Chem. Phys. 16, 9847–9862. https://doi.org/10.5194/acp-16-9847-2016.

Silva, R.A., West, J.J., Lamarque, J.-F., Shindell, D.T., Collins, W.J., Faluvegi, G., Folberth, G.A., Horowitz, L.W., Nagashima, T., Naik, V., Rumbold, S.T., Sudo, K., Takemura, T., Bergmann, D., Cameron-Smith, P., Doherty, R.M., Josse, B., MacKenzie, I.A., Stevenson, D.S., Zeng, G., 2017. Future global mortality from changes in air pollution attributable to climate change. Nat. Clim. Chang. 7, 647–651. https://doi.org/10.1038/nclimate3354.

Soares, A.R., Silva, C., 2022. Review of ground-level ozone impact in respiratory health deterioration for the past two decades. Atmosphere (Basel) https://doi.org/10.3390/atmos13030434.

Tagaris, E., Liao, K.-J., Delucia, A., Deck, L., Amar, P., Russell, A., 2009. Potential impact of climate change on air pollution-related human health effects. Environ. Sci. Technol. 43, 4979–4988. https://doi.org/10.1021/es803650w.

Thornhill, G., Collins, W., Olivié, D., Skeie, B.R., Archibald, A., Bauer, S., Checa-Garcia, R., Fiedler, S., Folberth, G., Gjermundsen, A., Horowitz, L., Lamarque, J.F., Michou, M., Mulcahy, J., Nabat, P., Naik, V., O'Connor, M.F., Paulot, F., Schulz, M., Scott, E.C., Séférian, R., Smith, C., Takemura, T., Tilmes, S., Tsigaridis, K., Weber, J., 2021. Climate-driven chemistry and aerosol feedbacks in CMIP6 Earth system models. Atmos. Chem. Phys. 21, 1105–1126. https://doi.org/10.5194/acp-21-1105-2021.

Travis, K.R., Crawford, J.H., Chen, G., Jordan, C.E., Nault, B.A., Kim, H., Jimenez, J.L., Campuzano-Jost, P., Dibb, J.E., Woo, J.-H., Kim, Y., Zhai, S., Wang, X., McDuffie, E.E., Luo, G., Yu, F., Kim, S., Simpson, I.J., Blake, D.R., Chang, L., Kim, M.J., 2022. Limitations in representation of physical processes prevent successful simulation of PM2.5 during KORUS-AQ. Atmos. Chem. Phys. 22, 7933–7958. https://doi.org/10.5194/acp-22-7933-2022.

Turnock, S.T., Allen, R.J., Andrews, M., Bauer, S.E., Deushi, M., Emmons, L., Good, P., Horowitz, L., John, J.G., Michou, M., Nabat, P., Naik, V., Neubauer, D., O'Connor, F.M., Olivié, D., Oshima, N., Schulz, M., Sellar, A., Shim, S., Takemura, T., Tilmes, S., Tsigaridis, K., Wu, T., Zhang, J., 2020. Historical and future changes in air pollutants from CMIP6 models. Atmos. Chem. Phys. 20, 14547–14579. https://doi.org/10.5194/acp-20-14547-2020.

van Marle, M.J.E., Kloster, S., Magi, B.I., Marlon, J.R., Daniau, A.-L., Field, R.D., Arneth, A., Forrest, M., Hantson, S., Kehrwald, N.M., Knorr, W., Lasslop, G., Li, F., Mangeon, S., Yue, C., Kaiser, J.W., van der Werf, G.R., 2017. Historic global biomass burning emissions for CMIP6 (BB4CMIP) based on merging satellite observations with proxies and fire models (1750–2015). Geosci. Model Dev. 10, 3329–3357. https://doi.org/10.5194/gmd-10-3329-2017.

Xu, J., Yao, M., Wu, W., Qiao, X., Zhang, H., Wang, P., Yang, X., Zhao, X., Zhang, J., 2021. Estimation of ambient PM2.5-related mortality burden in China by 2030 under climate and population change scenarios: a modeling study. Environ. Int. 156. https://doi.org/10.1016/j.envint.2021.106733.

Yorifuji, T., Bae, S., Kashima, S., Tsuda, T., Doi, H., Honda, Y., Kim, H., Hong, Y.-C., 2015. Health impact assessment of PM10 and PM2.5 in 27 southeast and East Asian cities. J. Occup. Environ. Med. 57, 751–756. https://doi.org/10.1097/JOM.0000000000000485.

Zhai, S., Jacob, D., Shah, V., Yang, L., Zhang, Q., Sun, Y., Wang, S., Luo, G., Yu, F., Woo, J.-H., Kim, Y., Kim, H., Dibb, J., Lee, T., Han, J.-S., Li, K., Liao, H., 2022. Coarse Particulate Matter Air Quality in East Asia: Implications for Fine Particulate Nitrate.

Update

Science of the Total Environment

Volume 964, Issue , 10 February 2025, Page

DOI: https://doi.org/10.1016/j.scitotenv.2025.178553

Science of the Total Environment 964 (2025) 178553

Contents lists available at ScienceDirect

Science of the Total Environment

journal homepage: www.elsevier.com/locate/scitotenv

Corrigendum

Corrigendum to "Future air quality and premature mortality in Korea" [Science of the Total Environment 865 (2023) 161134]

Yujin J. Oak [a], Rokjin J. Park [a,*], Jong-Tae Lee [b,c], Garam Byun [c]

[a] School of Earth and Environmental Sciences, Seoul National University, Seoul, South Korea
[b] School of Health Policy and Management, College of Health Science, Korea University, Seoul, South Korea
[c] Interdisciplinary Program in Precision Public Health, Korea University, Seoul, South Korea

The authors regret that the wrong supplementary file has been uploaded. Here we provide the supplementary figures (Fig. S1-S4). The authors would like to apologize for any inconvenience caused.

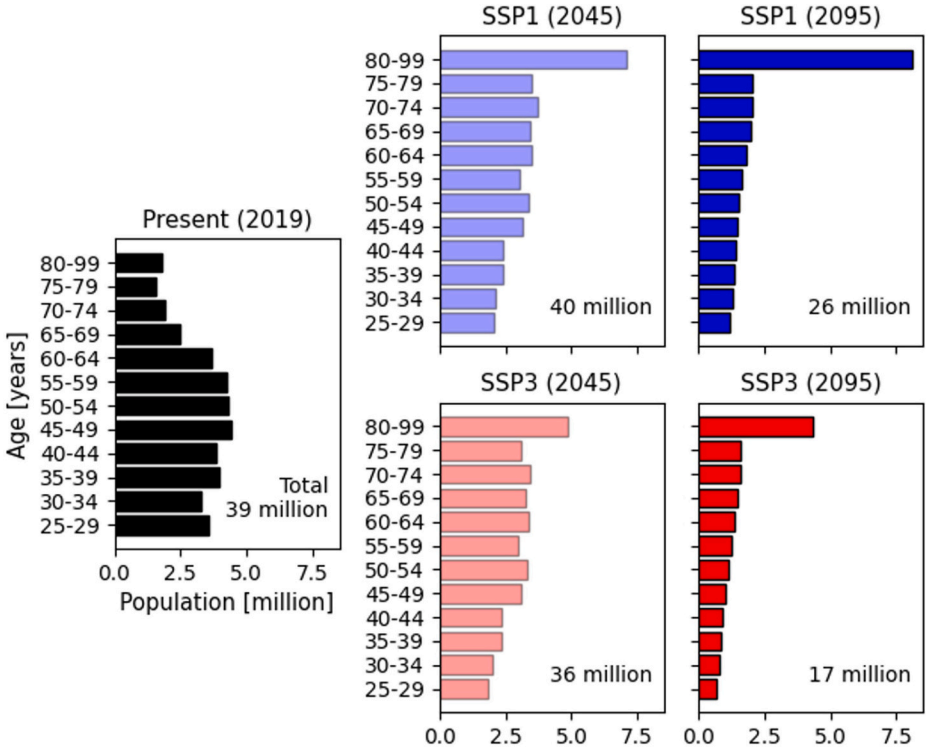

Fig. S1. Age structure of total adult (25 ≥ years) population in Korea in 2019, and projected age structures for 2045 and 2095 under SSP1 and SSP3. Total adult population sizes are denoted in the lower-right corners.

DOI of original article: https://doi.org/10.1016/j.scitotenv.2022.161134.
* Corresponding author.
E-mail address: rjpark@snu.ac.kr (R.J. Park).

https://doi.org/10.1016/j.scitotenv.2025.178553

Available online 24 January 2025

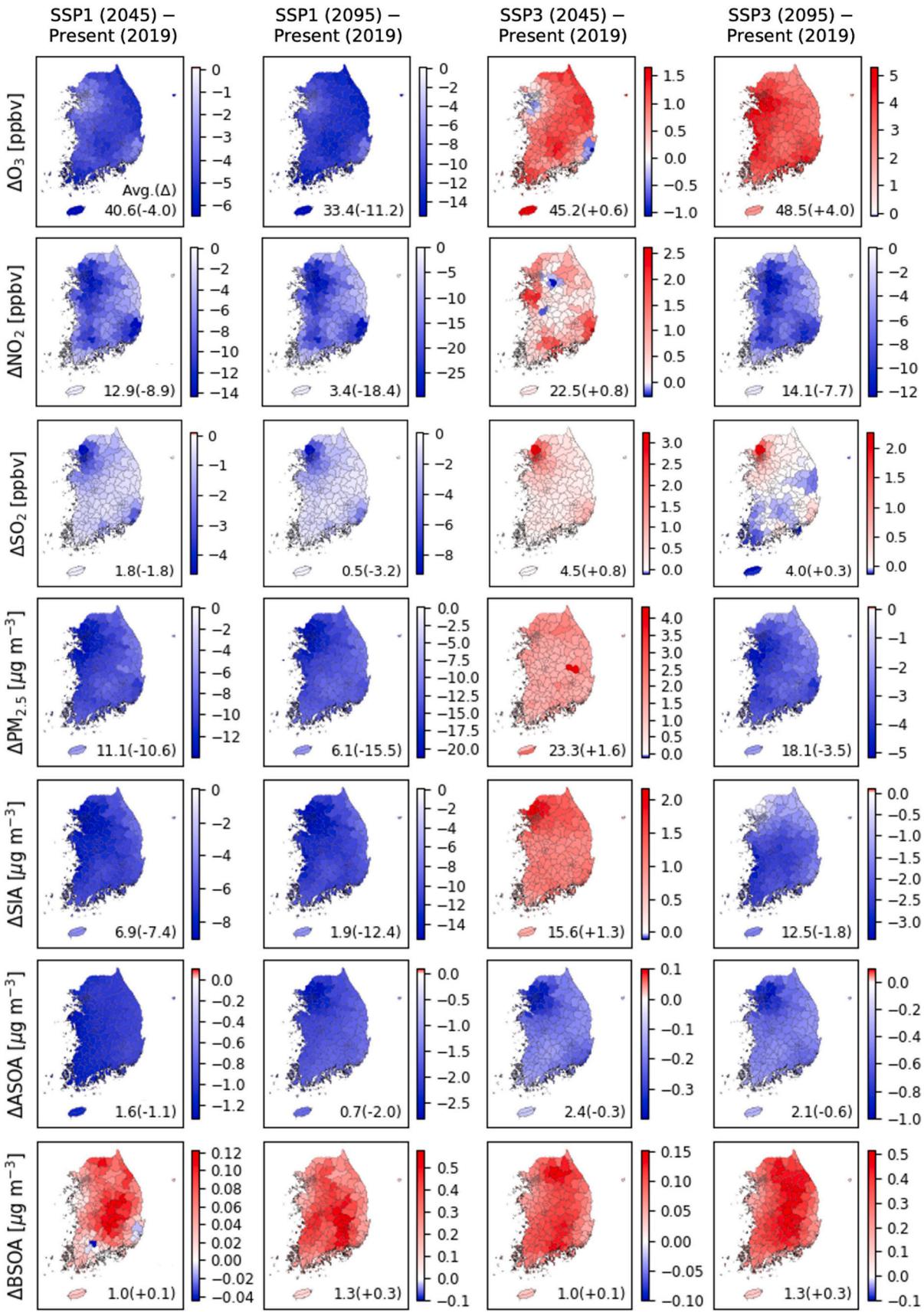

Fig. S2. Future changes in simulated annual mean concentrations of gas (O_3, NO_2, SO_2) and aerosol ($PM_{2.5}$, SIA, ASOA, BSOA) species in Korea. The average concentrations (Avg.) under each scenario and changes (Δ) relative to present conditions are denoted in the lower-right corners.

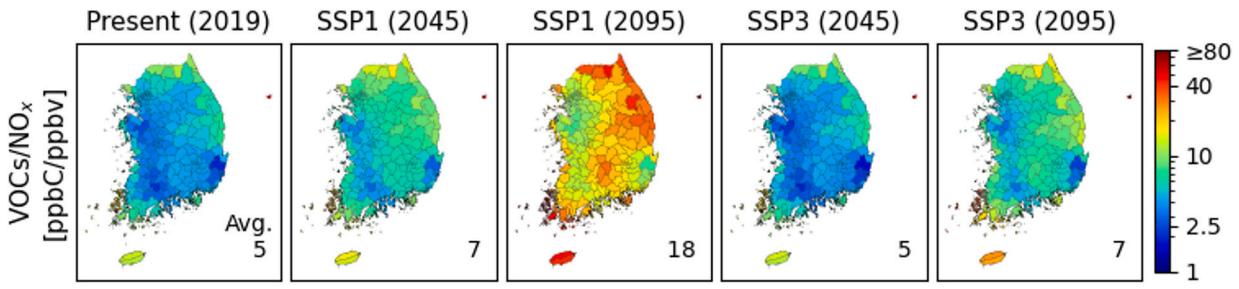

Fig. S3. Simulated annual mean VOCs/NO_x ratios in the present, near-term, long-term future under SSP1 and SSP3 in Korea. The average values (Avg.) are denoted in the lower-right corners.

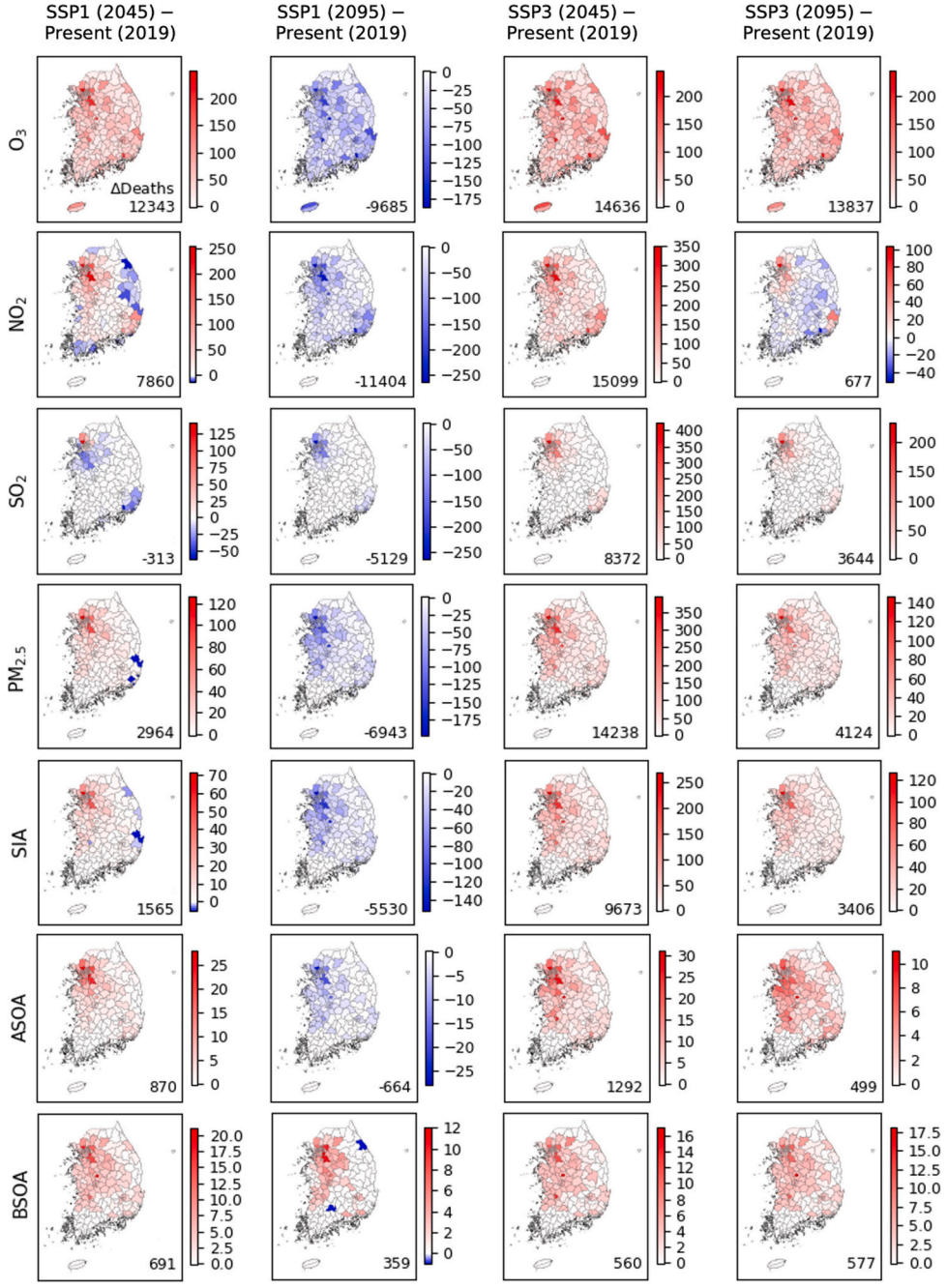

Fig. S4. Future changes in estimated premature mortality due to O_3, NO_2, SO_2, $PM_{2.5}$, SIA, ASOA, and BSOA exposure in Korea. The changes in total deaths (ΔDeath) relative to present conditions are denoted in the lower-right corners.